

1 Stress testing insurance market stability under 2 climate risk

3 Simona Meiler^{1,*}, Steven I. Jackson², Kerry Emanuel³, Noah S. Diffenbaugh⁴, and Jack W.
4 Baker¹

5 ¹Civil and Environmental Engineering, Stanford University, CA, USA

6 ²American Academy of Actuaries, Washington, DC, USA

7 ³Lorenz Center, Massachusetts Institute of Technology, Cambridge, Massachusetts, USA

8 ⁴Earth System Science, Stanford University, CA, USA

9 *Corresponding author: simona@simonameiler.ch

10 *This manuscript is a non-peer-reviewed preprint submitted to EarthArXiv and currently under review. The content has not yet*
11 *been certified by peer review and may be subject to change.*

12 ABSTRACT

13 Climate change, urban development, and evolving insurance markets threaten the stability of disaster-risk financing. Homeown-
14 ers insurance is embedded in a layered network of reinsurers, capital markets, and public backstops that absorb losses and
15 can be overwhelmed by extreme events. We develop a probabilistic risk-propagation model linking physics-based simulations
16 of tropical cyclone wind and flood losses to residential insurance markets, backstop mechanisms, and regulatory thresholds,
17 applied to Florida under present-day and future climate conditions. Between 10- and 100-year tropical cyclone seasons, total
18 losses increase ninefold while public burden increases more than fortyfold as institutional thresholds and capital constraints bind.
19 Post-insolvency mechanisms, residual markets, and the National Flood Insurance Program are more sensitive to extreme events
20 than the reinsurance layer, and this concentration intensifies under climate change. The framework provides a transferable
21 template for stress-testing insurance systems and evaluating how climate change, market dynamics, and adaptation reshape
22 systemic disaster risk.

23 Introduction

24 The 2017 hurricane season (Harvey, Irma, Maria) generated more than USD 260 billion in total losses, or the equivalent of
25 7–14% of global reinsurers' capital, and absorbed the industry's net income for the year (1). The increasing likelihood of
26 many weather and climate extremes (2) and compound events (3) erodes the stationarity that underpins traditional disaster risk
27 assessment and pricing (4). What was previously manageable year-to-year volatility increasingly reflects systematic changes
28 in hazard characteristics, with implications for long-term planning, capital allocation, and financial stability (5, 6). Disaster
29 insurance transfers losses from households to insurers and state-backed providers, allowing post-disaster repair, supporting
30 mortgage markets, and accelerating economic recovery after extreme events (4, 7). Primary insurers absorb losses up to their
31 capital and reinsurance protection, after which risks propagate to reinsurers, catastrophe bond investors, and public backstops
32 such as state insurance programs or federal institutions. Under moderate shocks, this structure spreads risk efficiently; however,
33 under extreme or clustered events, contractual limits, capital constraints, and regulatory thresholds can bind, causing losses to
34 cascade across institutions rather than being smoothly absorbed (8–10).

35 In California and Florida, continued urban development (11, 12) and repeated wildfire and tropical cyclone (TC) losses have
36 led to insurer withdrawals, insolvencies, rapid premium increases, and growing reliance on residual or state-backed markets
37 (13–16). In both cases, risk increasingly shifts back to households and public institutions beyond the scale for which these
38 mechanisms were designed, raising concerns that climate-driven disasters may transition from diversifiable shocks to systemic
39 insurance market stress.

40 Despite growing recognition that climate-driven disasters pose systemic financial risks, insurance markets lack quantitative
41 system-wide stress tests of the kind used to assess stability in banking. In the banking sector, stress testing is a central tool
42 for evaluating the resilience of complex financial systems to rare but severe shocks, focusing on tail risks and the potential
43 for cascading failures (17–19). Climate-related scenario analysis has since been incorporated into prudential supervision,
44 including central bank and regulatory stress-testing exercises (20–22). By contrast, climate risk assessments in insurance have
45 largely centered on catastrophe loss reporting, disclosure frameworks, and firm-level solvency exercises (23–26), which are not

designed to quantify when aggregate losses overwhelm market-wide capacity, trigger public backstops, or propagate across interconnected private and public actors. This gap is increasingly consequential as climate change shifts the frequency and clustering of extreme events.

Here, we develop a probabilistic, system-wide stress-testing framework that quantifies the probability of systemic insurance failure by propagating losses through primary insurers, reinsurers, capital markets, and public institutions, as contractual limits, capital constraints, and statutory thresholds are reached. We apply this framework to the Florida residential property insurance market, where high exposure to TCs, dense coastal development (27), and recent insurer insolvencies (28) following Hurricane Ian make systemic risk an immediate concern (10). We simulate losses from historical TCs (29), stylized sequential events, and large probabilistic event sets representing present-day and future climate conditions (30, 31), and examine how evolving market conditions and adaptation measures modify systemic risk (Fig. 1).

Florida's residential insurance system absorbs TC losses through three sequential layers. Losses are first distributed across private wind insurers, Citizens Property Insurance Corporation (Florida's state-created insurer of last resort), the National Flood Insurance Program (NFIP), and uninsured or underinsured households. Insured losses are then partially redistributed through reinsurance via the Florida Hurricane Catastrophe Fund (FHCF) and catastrophe bonds. When insurer capital or public insurance resources are exhausted, institutional backstops activate: Florida Insurance Guaranty Association (FIGA) assessments on surviving insurers, tiered Citizens assessments on Citizens and statewide policyholders, and Treasury borrowing to cover NFIP shortfalls. Our analysis tracks losses through each layer to quantify household exposure, insurer stress, and the resulting public burden. Florida is an early manifestation of climate-related insurance stress (10). While institutional details vary across regions and hazards, layered risk transfer is a common feature of disaster insurance systems. Our framework provides a transferable approach for identifying where extreme losses accumulate, under which conditions private capacity is overwhelmed, and how policy interventions reshape systemic risk.

Results

Stress testing the insurance system with historical and sequential events

We examine how extreme losses are distributed across households, insurers, and public backstops, using four historically damaging TCs affecting Florida: the Great Miami Hurricane (1926), the Lake Okeechobee Hurricane (1928), Hurricane Andrew (1992), and Hurricane Irma (2017), as well as paired and repeated-event scenarios, evaluated on 2024 exposure and insurance market conditions. Modeled total losses (table S3) fall within the range of published normalized estimates (32, Supplementary Material Table 2).

Across all scenarios, approximately 60–75% of losses remain uninsured or underinsured (Fig. 2a), with the highest shares occurring in flood-heavy events affecting inland areas with low flood insurance penetration (Fig. 1a, right-most panel). Public burden — residual losses propagated through the insurance system to public institutions after private capital and statutory backstop capacities are exhausted — reaches approximately USD 12 billion for Hurricane Andrew, USD 18 billion for the Lake Okeechobee Hurricane, and USD 26 billion for the Great Miami Hurricane. Sequential events generate public burdens of USD 50–65 billion, exceeding the sum of individual-event burdens: a nonlinear amplification of public costs reflecting institutional thresholds and payout caps. By contrast, Hurricane Irma losses are largely absorbed by the initial insurance layers (public burden of USD 0.2 billion). Although the FHCF only reaches its statutory cap for Great Miami-scale or sequential events, FIGA, Citizens, and the NFIP accrue deficits in most scenarios that would require multiple years of premium income to recover (table S3, stress ratios).

Probabilistic assessment of systemic insurance risks

Moving beyond individual scenarios, we quantify systemic insurance risk probabilistically using a catalog of 10000 simulated TC seasons (Section Hazard and loss modeling). Table 1 places the scenario-based stress tests into a probabilistic context by reporting seasonal return period estimates under present-day climate conditions. A total seasonal loss comparable to the Great Miami Hurricane (\approx USD 170 billion) corresponds to a return period of approximately 35 years under present-day climate and exposure, while the sequential-event scenarios examined above approach the magnitude of a 100-year season.

Moreover, the probabilistic results reveal pronounced nonlinear amplification of public burden with increasing loss severity. While total seasonal losses increase by roughly a factor of nine between the 10-year and 100-year seasons (USD 39.5 to 357.2 billion), total public burden increases by over a factor of forty (USD 1.7 to 74.0 billion; Table 1). This supralinear scaling reflects exhaustion of private insurer capital, activation of institutional thresholds, and binding payout caps that shift an increasing share of losses to public and quasi-public backstops in the tail of the distribution.

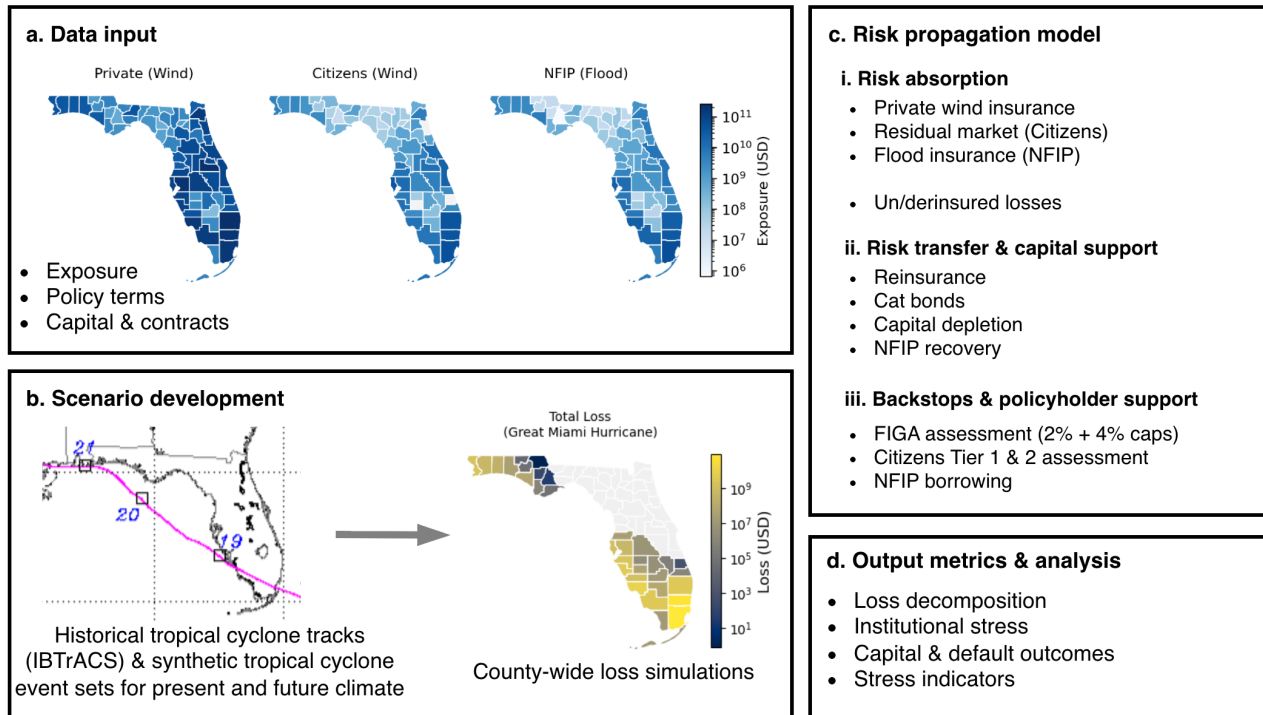


Fig. 1. Insurance system architecture and risk propagation in the Florida homeowners' property insurance market. a) County-level exposure and coverage-in-force for private wind insurers, Citizens Property Insurance Corporation, and the U.S. National Flood Insurance Program (NFIP), together with policy terms, capital positions, and contractual constraints. b) Historical tropical cyclone tracks (IBTrACS) and synthetic event sets representing present and future climate conditions translated into county-level wind and flood loss simulations. c) Loss propagation across three layers: (i) initial risk absorption by insurers, Citizens, the NFIP, and under- or uninsured households; (ii) redistribution through reinsurance, catastrophe bonds, and capital depletion; and (iii) activation of institutional backstops and policyholder assessments, including the Florida Hurricane Catastrophe Fund (FHCF), Florida Insurance Guaranty Association (FIGA), Citizens assessments, and NFIP borrowing. d) Output metrics capturing loss decomposition, insurer capital depletion and defaults, activation of public backstops, and system-level stress indicators under single, sequential, and probabilistic event scenarios.

95 Across return periods, FIGA residuals constitute the largest and fastest-growing component of public burden. In a 100-year
 96 season, FIGA residual losses (USD 32.8 billion) account for nearly half of the total public burden, exceeding both Citizens
 97 deficits (USD 17.2 billion) and NFIP borrowing (USD 10.3 billion). FIGA remains the dominant channel through which
 98 losses enter quasi-public balance sheets across the full range of return periods considered, whereas FHCF shortfalls remain
 99 comparatively limited and occur primarily in more extreme seasons.

100 The probabilistic approach further allows us to assess the annual exceedance probability of systemic risk thresholds that
 101 indicate stress across different components of the insurance system (Fig. 3a, table S5). For the private wind insurance market,
 102 the annual probability of more than ten insurer defaults is 11.4%, while the probability that the single largest company deficit
 103 exceeds USD 1 billion is 7.2%.

104 For public and quasi-public institutions, the annual probability of exceeding capacity or statutory thresholds differs across
 105 entities. The probability that the FHCF reaches its statewide seasonal payout cap is 0.8%, whereas the probabilities of FIGA
 106 and Citizens exceeding their respective assessment capacities are 13.6% and 9.5%. For the NFIP, the probability that annual
 107 losses exceed twice its annual premium income is 5.0%. These results mirror the scenario-based findings in Fig. 2, highlighting
 108 comparatively greater vulnerability of FIGA, Citizens, and the NFIP relative to the FHCF.

109 Finally, we relate the aggregate public burden to the economic scale of Florida. The annual probability that total public
 110 burden exceeds 1% of Florida's GDP is 3.7%, while the probability of exceeding 10% of state GDP is 0.1%.

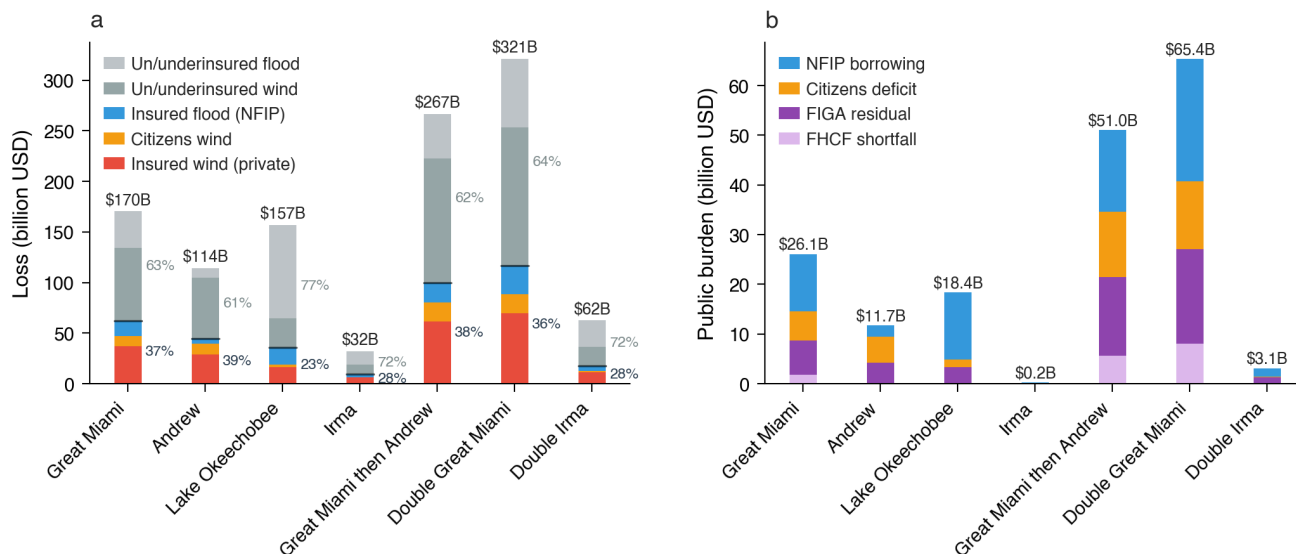


Fig. 2. Loss decomposition and public burden across historical and sequential TC scenarios. a) Decomposition of total losses across insured wind (private market and Citizens), insured flood, and uninsured or underinsured losses. The black horizontal line indicates the split between insured and uninsured losses, with corresponding shares shown numerically. b) Public burden after exhaustion of private insurer capital and risk-transfer mechanisms, apportioned across key public backstops. Total loss and public burden values (USD B) are shown above each bar. All values are shown for single and sequential-event scenarios; a complete tabulation, including uncertainty ranges, is provided in table S3.

Systemic risk probabilities increase with climate change

We next evaluate how projected changes in TC hazard alter systemic insurance risk, holding exposure, capital positions, and regulatory parameters at present-day values. Projections span mid-century (2041–2060) and end-of-century (2081–2100) under SSP2-4.5 and SSP5-8.5 emission scenarios. Future changes are estimated using a multi-model delta approach: ensemble-median changes in each risk metric across five CMIP6 simulations are added to the ERA5-based present-day baseline (Section [Future climate scenarios](#)).

Under mid-century scenarios (2041-2060), expected annual total losses approximately double relative to present-day conditions, and expected public burden increases by a factor of approximately three (table S4). Exceedance probabilities of several systemic stress thresholds increase across the private market and post-insolvency channels (Fig. 3, table S5). The annual probability of more than ten insurer defaults rises from 11.4% under present-day conditions to 17.7% (SSP2-4.5) and 18.8% (SSP5-8.5).

Post-default and residual-market mechanisms exhibit particularly strong amplification. The probability that FIGA exceeds its statutory assessment capacity increases from 13.6% to 22.1–23.3%, while Citizens exceeds its assessment capacity with probabilities rising from 9.5% to 15.1–16.1%. In contrast, the probability that the FHCF reaches its statewide payout cap remains at or below 1% across scenarios, and the probability that NFIP annual losses exceed twice premium income increases only modestly (from 5.0% to 5.9–6.1%).

Uncertainty across climate models is substantial but does not alter the qualitative direction of change (table S5). Under 2050 SSP5-8.5, the probability that FIGA exceeds capacity ranges from 16.6% to 30.9% across the GCM ensemble, compared with 13.2–14.1% at baseline, with similar spreads for private insurer defaults and Citizens deficits. Differences between emission scenarios widen by end-of-century but remain smaller than the inter-GCM range. At the aggregate level, the annual probability that total public burden exceeds 1% of Florida’s GDP increases modestly from 3.7% to 4.3–4.5% by mid-century, while exceedance of 10% of GDP remains rare.

Systemic risks with evolving markets and insurance policies

We next evaluate how changes in market structure and insurance policies modify systemic risk under present-day hazard conditions. The three stylized interventions represent dynamics currently discussed in policy and industry debates: private-market contraction and expansion of residual markets following recent insolvencies and insurer withdrawals (13, 15, 16);

Table 1. Loss decomposition and public institutional burden across return periods. Return period (RP) estimates are shown for total losses, their decomposition across insured and uninsured components, and the resulting public and quasi-public institutional burden. Public burden reflects residual financial obligations borne by public backstops after exhaustion of private insurer capital and risk-transfer mechanisms.

Metric (USD B)	Return period [years]						
	10	25	50	100	250	500	1000
<i>Loss decomposition</i>							
Total loss	39.5	146.9	246.4	357.2	563.9	628.0	738.0
Insured wind – private	11.6	41.8	69.7	103.2	155.2	198.4	214.3
Citizens wind	1.8	6.8	14.5	22.1	35.6	53.6	62.9
Insured flood – NFIP	0.9	3.7	7.4	13.7	26.1	37.6	50.3
Un/underinsured wind	19.8	71.8	125.9	183.1	257.6	321.1	392.1
Un/underinsured flood	3.9	15.1	28.4	47.1	87.3	112.7	141.7
<i>Institutional stress</i>							
Total public burden	1.7	13.9	39.6	74.0	127.7	180.9	214.3
FHCF shortfall	0.0	0.0	6.5	13.7	20.8	26.8	29.6
FIGA residual	1.0	9.2	19.2	32.8	54.9	72.8	80.6
Citizens deficit	0.7	4.5	9.9	17.2	29.3	47.3	57.2
NFIP Treasury borrowing	0.0	0.2	4.0	10.3	22.7	34.1	46.8

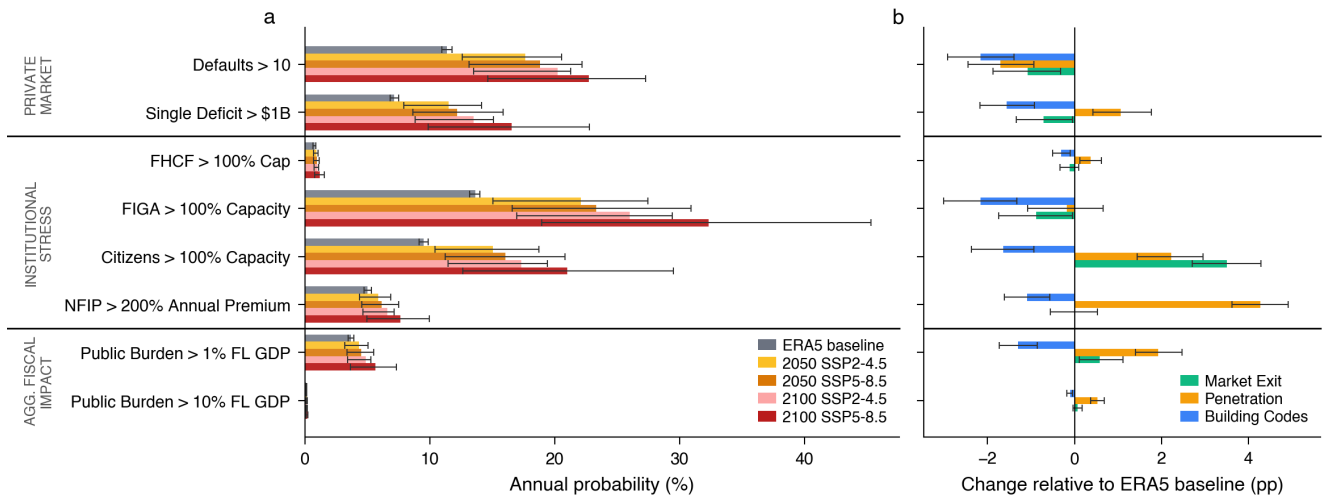


Fig. 3. Probabilistic assessment of systemic insurance risks under future climate scenarios and stylized policy interventions. Annual exceedance probabilities of predefined systemic stress thresholds across the private insurance market (top), public and quasi-public entities (middle), and aggregate fiscal impact measured as total public burden relative to Florida’s GDP (bottom). (a) Absolute annual exceedance probabilities under present-day and future climate conditions. Shown are results for the ERA5 baseline climate (grey), mid-century SSP2-4.5 (yellow) and SSP5-8.5 (orange), and end-of-century SSP2-4.5 (pink) and SSP5-8.5 (red). Bars show mean annual exceedance probabilities corresponding to the median climate-induced risk change across the GCMs used for tropical cyclone track set generation (Section [Future climate scenarios](#)), based on 10000 simulated tropical cyclone seasons; error bars indicate the 10th–90th percentile range across the full GCM ensemble. (b) Changes in annual exceedance probabilities relative to the ERA5 baseline configuration under three stylized policy scenarios: private insurer market exit (green), increased insurance penetration (orange), and strengthened building codes (blue). Values represent percentage-point changes under present-day hazard conditions. Bars show mean changes based on 10000 simulated tropical cyclone seasons, with error bars indicating the 10th–90th percentile. Positive values indicate an increase in the probability of exceeding the corresponding stress threshold relative to baseline; negative values indicate a reduction.

137 expansion of insurance penetration to reduce protection gaps (10); and strengthened building codes and retrofitting initiatives
 138 aimed at reducing physical losses (33, 34). Each intervention modifies a distinct layer of the insurance system architecture
 139 while holding all other model components constant (Section [Stylized market and policy interventions](#)).

140 **Private insurer market exit** We model a contraction of the private wind market that increases Citizens' market share from
 141 15% to 25% of total insured value, corresponding to a 10% shift of exposure from private insurers, of which 85% transfers to
 142 Citizens and 15% becomes uninsured. Under this scenario, the annual probability of more than ten private insurer defaults
 143 declines by about 1.1 percentage points relative to the ERA5 baseline (Fig. 3b, table S5), reflecting the reduced exposure
 144 and insured loss volume within the private market. However, systemic stress shifts toward residual market mechanisms. The
 145 probability that Citizens exceeds its assessment capacity increases by about 3.5 percentage points, while exceedance of the
 146 FHCF statewide payout cap remains nearly unchanged (table S5). Expected total public burden rises from USD 2.7 billion to
 147 USD 3.1 billion (table S4), and the probability that total public burden exceeds 1% of Florida's GDP increases by around 0.6
 148 percentage points (Fig. 3b, table S5).

149 **Insurance penetration increase** We increase wind (from 40% to 60%) and flood (from 11% to 30%) penetration rates, with
 150 insurer surplus and NFIP premium volumes scaling proportionally to insured exposure. While expanded coverage reduces
 151 uninsured losses from USD 12.1 billion (combined wind and flood) under baseline conditions to USD 7.8 billion (table S4), its
 152 systemic effects are heterogeneous. Several indicators of stress in public or quasi-public institutions increase under higher
 153 insurance penetration. Most notably, the annual probability that NFIP losses exceed 200% of annual premium income increases
 154 by 4.3 percentage points relative to the ERA5 baseline (Fig. 3b, table S5), despite the proportional expansion of the premium
 155 base — reflecting both the geographic concentration of the new exposure and the supralinear growth of tail losses relative to
 156 mean losses under correlated risk. The probability that Citizens exceeds its assessment capacity increases by 2.3 percentage
 157 points, and the probability that total public burden exceeds 1% of Florida's GDP increases by 1.9 percentage points (table S5).
 158 Expected public burden rises from USD 2.7 billion to USD 5.1 billion (table S4).

159 In contrast, several indicators of stress within the private insurance market decline. The annual probability of more than ten
 160 private insurer defaults decreases by 1.7 percentage points, while FIGA exceedance decreases marginally by 0.2 percentage
 161 points (table S5). These patterns indicate that proportional scaling of capital and premium income does not automatically
 162 preserve institutional resilience when insured loss volumes increase (Section [Stylized market and policy interventions](#)).

163 **Building code improvement** We reduce wind-related losses by 30% and flood-related losses by 25% relative to baseline
 164 vulnerability before allocation across institutional layers. Exceedance probabilities decline consistently across private, residual,
 165 and public components (Fig. 3b, table S5). The annual probability of more than ten private insurer defaults decreases by 2.2
 166 percentage points relative to the ERA5 baseline, FIGA exceedance decreases by 2.1 percentage points, and Citizens capacity
 167 exceedance decreases by 1.6 percentage points. The probability that total public burden exceeds 1% of Florida's GDP declines
 168 by 1.3 percentage points (table S5). Expected total public burden decreases from USD 2.7 billion to USD 1.6 billion (table S4).
 169 Unlike the redistribution scenarios above, structural mitigation reduces systemic stress simultaneously across all layers of the
 170 insurance architecture.

171 We next quantify the building code-related loss reduction required to offset projected mid-century climate impacts (SSP2-4.5,
 172 2041-2060) and restore systemic risk metrics to their present-day ERA5 baseline values (Figure 4). For the GCM ensemble
 173 median, annual total losses and total public burden respond approximately linearly to mitigation intensity, while insurer defaults
 174 respond more nonlinearly, with sharper reductions beyond about 70% loss mitigation. Combined wind and flood loss reductions
 175 of 70-75% are required to restore systemic risk metrics to baseline. The required reduction is sensitive to hazard uncertainty,
 176 ranging from 30-40% under lower-end GCM projections to 75-80% at the upper end.

177 Discussion

178 Public and quasi-public financial burdens scale disproportionately relative to primary disaster losses as institutional thresholds
 179 and capital constraints bind. Across probabilistic simulations of Florida's 2024 insurance market, total seasonal losses increase
 180 by approximately a factor of nine between 10-year and 100-year return period seasons, while total public burden increases by a
 181 factor of over forty (Table 1). Previous analyses have suggested nonlinear amplification qualitatively (15); our probabilistic
 182 framework quantifies it.

183 This amplification of public burden is also unevenly distributed across institutions. The highest systemic stress falls on
 184 FIGA, followed by Citizens and the NFIP. The annual probability of exceeding institutional capacity or statutory thresholds
 185 reaches 13.6% for FIGA and 9.5% for Citizens (Fig. 3a). In contrast, the FHCF remains comparatively resilient across
 186 baseline, climate change, and market adaptation scenarios, with a consistently low probability of reaching its statutory cap. The

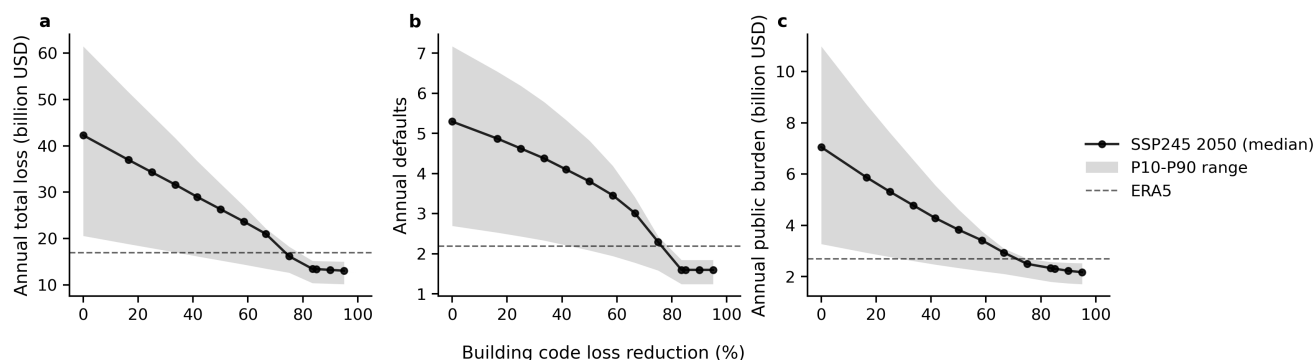


Fig. 4. Sensitivity of systemic insurance outcomes to building code-related loss reductions under future climate conditions. Sensitivity analysis showing the effect of incremental reductions in wind- and flood-related losses resulting from strengthened building codes on systemic risk outcomes under mid-century (2041-2060) SSP2-4.5 climate conditions. Shown are a) annual total loss, b) annual number of private insurer defaults, and c) annual total public burden. Solid lines indicate results for the median climate-induced risk change across the GCM ensemble, shaded bands show the 10th–90th percentile range across GCMs, and dashed lines denote the present-day ERA5 baseline. All quantities represent mean annual outcomes across 10000 simulated tropical cyclone seasons per climate realization.

187 13.6% annual exceedance probability for FIGA corresponds to approximately a 1-in-7-year frequency of FIGA exhausting its
 188 assessment capacity — more than three times more frequent than Andrew-level losses, whose return period under the 2024
 189 Florida market configuration is less than 25 years (Table 1). Both examples are thus matters of immediate concern, not rare
 190 tail-risk scenarios.

191 Because interventions are evaluated within the same architecture, their effects propagate through the entire insurance
 192 system. Increasing insurance penetration with proportional capital expansion, for example, reduces private-insurer stress but
 193 raises public backstop exposure: the annual probability that NFIP losses exceed 200% of annual premium income rises by 4.3
 194 percentage points, and Citizens capacity exceedance rises by 2.3 percentage points (Section [Insurance penetration increase](#)).
 195 Policies targeting one component of the insurance market can thus redistribute systemic risk across institutions rather than
 196 uniformly reducing it.

197 The market dynamics and policy interventions examined here are stylized and designed to probe systemic sensitivity rather
 198 than forecast specific outcomes. Empirical evidence suggests that strengthened building codes can reduce hurricane-related
 199 wind damage by approximately 30–50% relative to pre-code construction (33, 35). But offsetting increases in systemic risk
 200 projected for the mid-century (2050, SSP2-4.5) would require loss reductions of approximately 70–75% under the median
 201 hazard scenario. These required reductions exceed empirically observed performance improvements but fall within plausible
 202 bounds under less severe hazard realizations within our mid-century ensemble (Fig. 4). This spread reflects differences in
 203 climate sensitivity across the underlying GCMs (36), and suggests that reliance on a single structural measure is unlikely to
 204 suffice under stronger warming. Instead, a portfolio of complementary policy and market interventions may be required to
 205 strengthen insurance market resilience.

206 Several caveats bound the interpretation of these results. The analysis focuses on Florida and on tropical cyclones; the
 207 FHCF is the only reinsurance mechanism explicitly represented, and statewide private-insurer market shares are disaggregated
 208 uniformly to counties — both choices that likely overstate modeled insurer defaults and FIGA assessments. The 2024 market
 209 architecture is held fixed across future climate scenarios, so future stress estimates should be interpreted as conditional
 210 assessments of the present-day market configuration rather than forecasts of how the market will actually evolve. Sea-level
 211 rise is not explicitly included in future hazard sets, implying that long-term flood-related systemic risks may be conservatively
 212 estimated. Each of these caveats can be relaxed in future applications of the framework.

213 By embedding probabilistic hazard realizations within a market-wide representation of insurer capitalization and public
 214 backstops, this study provides a quantitative framework for evaluating how climate-driven disaster losses propagate through
 215 insurance systems. Our results show that systemic financial exposure can increase nonlinearly with disaster losses, concentrate
 216 within specific public backstop institutions, and shift across actors in response to policy and market changes. These findings
 217 highlight the importance of system-wide stress testing approaches that capture institutional thresholds and interactions when
 218 assessing the financial stability implications of climate risk.

219 Beyond Florida, the framework developed here provides a template for stress-testing other climate-exposed insurance
220 markets. California’s wildfire-prone regions (37) reflect the same layered risk-transfer vulnerabilities shown here, and similar
221 risk-transfer markets govern disaster insurance internationally. A key priority for future research is to trace how uninsured losses
222 propagate into housing markets, credit systems, and public finance, where emerging evidence points to climate-driven debt
223 feedbacks at the municipal level (38) and persistent protection gaps across U.S. flood markets (39). Developing integrated tools
224 that capture these cross-sector feedbacks will be essential for managing climate risk in increasingly interconnected financial
225 and economic systems.

226 Methods

227 Data

228 **Insurance market data**

229 Insurance market inputs are anchored to statutory and financial conditions as of 2024, based on insurer statutory filings,
230 regulatory reports, and administrative exposure datasets. Exposure and capital data are harmonized to the county level to ensure
231 consistency with aggregated TC loss estimates and are held constant across simulations.

232 **Exposure and coverage** For the private admitted market, total insured value (TIV) by county is obtained from the Florida
233 Hurricane Catastrophe Fund (FHCF) 2024 annual exposure report (40), which provides aggregate residential wind exposure
234 across all participating private insurers. To assign this county-level private TIV to individual insurers, we disaggregate it across
235 the top 100 individual insurers in proportion to their statewide residential direct premiums written for calendar year 2024, as
236 reported in statutory filings (NAIC annual statements, accessed via S&P Capital IQ) and Florida Office of Insurance Regulation
237 (FLOIR) market share reports (41). This procedure preserves observed statewide market structure while ensuring consistency
238 with county-level loss aggregation. Due to lack of alternative data, private insurers' county-level market shares are distributed
239 uniformly from statewide data, likely producing upper-bound estimates of company defaults.

240 Citizens Property Insurance Corporation's (hereafter, "Citizens") county-level wind exposure is obtained directly from its
241 published policies-in-force and exposure data as of September 30, 2024 (42). We include all personal residential policy lines,
242 comprising multiperil homeowners and wind-only residential policies.

243 Flood exposure is based on National Flood Insurance Program (NFIP) coverage-in-force and written premium data for
244 policy year 2024, obtained from the Federal Emergency Management Agency (FEMA) OpenFEMA datasets (43). NFIP
245 participation rates reflect observed take-up inside and outside Special Flood Hazard Areas (SFHAs) (44).

246 **Capital and surplus** Private insurer capital is measured as statutory surplus as regards policyholders for calendar year 2024,
247 obtained from statutory financial statements filed with the National Association of Insurance Commissioners (NAIC) and
248 accessed via S&P Capital IQ. For insurers affiliated with larger groups, both entity-level and group-level surplus are recorded
249 to allow for potential intragroup capital support within the risk propagation model (Section [Capital depletion and intragroup](#)
250 [support](#)).

251 Citizens' surplus as regards policyholders corresponds to its 2024 annual statutory financial statement (45).

252 NFIP capital consists of the combined National Flood Insurance Fund and Reserve Fund balance of USD 3.441 billion as of
253 October 28, 2024 (CRS Insights IN10784 (46)). Florida-specific annual written premium for policy year 2024, obtained from
254 FEMA OpenFEMA data (43), is used to define exceedance thresholds relative to annual premium income (Section [Output](#)
255 [metrics and stress indicators](#)).

256 **Reinsurance contracts and catastrophe bond data** FHCF contract parameters are based on the 2023–2024 reimbursement
257 contract year. Company-specific coverage elections (45%, 75%, or 90%), reimbursement premiums, and participating insurer
258 identifiers (NAIC codes) are obtained from FHCF coverage selections and premium calculation reports (40). Retention multiples
259 and coverage limits follow the statutory terms reported in the FHCF 2023–2024 annual report (47). Recoveries are subject to
260 the FHCF's season-wide statutory capacity limit of USD 17 billion. The FHCF is modeled as the only reinsurance mechanism
261 explicitly represented; private reinsurance not captured here could reduce modeled defaults and FIGA assessments.

262 Outstanding catastrophe bonds covering Florida wind exposure active during the 2024 hurricane season are identified using
263 the Artemis deal directory (48) and verified against sponsor offering documents and transaction disclosures. For each bond,
264 we extract sponsor, peril coverage, trigger type (indemnity, industry loss, or parametric), attachment point, exhaustion point,
265 and limit. Bonds are modeled as single-occurrence, single-season layers without reinstatements. Payouts are computed at the
266 sponsor level based on reported attachment and exhaustion terms.

267 **Tropical cyclone track data**

268 We use TC track data from two sources. Historical TC tracks are obtained from the International Best Track Archive for Climate
269 Stewardship (IBTrACS) (29). Synthetic TC tracks are generated using the statistical–dynamical MIT TC model (30, 31).

270 The model is forced with large-scale environmental fields from the European Centre for Medium-Range Weather Forecasts
271 (ECMWF) fifth-generation reanalysis (ERA5) (49) for present-day conditions and from five CMIP6 global climate models
272 (GCMs) for future conditions under SSP2-4.5 and SSP5-8.5 emission scenarios. The GCMs (CanESM5 (50), CNRM-CM6-1
273 (51), EC-Earth3 (52), IPSL-CM6A-LR (53), and MIROC6 (54)) span a broad range of global climate sensitivities. Simulations
274 cover three periods: a present-day reference (1980–2023 for ERA5; 1995–2014 for GCMs), mid-century (2041–2060), and
275 late-century (2081–2100). The model was used to generate 200 TCs for each year within these periods using the three-step

276 process of genesis, track, and intensity modeling, yielding a total of 8800 (ERA5) and 4000 (per GCMs) TCs per event
 277 set. Annual TC frequency emerges from the fraction of TC seeds used in the genesis step that develop into fully formed
 278 storms (>40 kn) under the prevailing environmental conditions (e.g., potential intensity, vertical wind shear). A frequency
 279 bias correction rescales the number of developed storms relative to the seeded ensemble, ensuring that simulated annual
 280 TC counts match the calibrated climatological baseline while preserving climate-driven variability across simulations. This
 281 frequency information is used to generate stochastic year sets (Section [Hazard and loss modeling](#)) and compute return periods
 282 (Section [Output metrics and stress indicators](#)).

283 To focus on Florida-relevant impacts, we retain only TC tracks passing within a 150 km coastal buffer of Florida.

284 **Hazard and loss modeling**

285 We compute county-level TC loss estimates from historical and synthetic TC tracks using the open-source, probabilistic climate
 286 risk modeling platform CLIMADA (55), which operationalizes the IPCC risk framework based on hazard, exposure, and
 287 vulnerability (56).

288 First, we use the Holland (2008) (57) parametric wind model to derive a two-dimensional wind field at a horizontal
 289 resolution of 120 arc-seconds (approximately 4 km at the equator) from each TC track. The wind model produces the gridded
 290 1-min average sustained winds at 10 m above ground, consisting of a circular wind field component and the translational wind
 291 speed generated by the TC's movement. In CLIMADA, the peak lifetime wind speed at each location is used as the hazard
 292 variable, disregarding values below 34 kn (17.5 ms^{-1}). We do not explicitly model TC rainfall or storm surge hazards; their
 293 relative contribution to total losses is incorporated through the wind-flood attribution approach described below (Section [Wind
 294 and flood loss estimation](#)). Sea-level rise projections are not included in future climate TC hazard sets.

295 Second, we derive a spatially explicit representation of gridded asset exposure values based on the LitPop method (58),
 296 which disaggregates national or subnational GDP values to a grid level based on nightlight intensity and population data. The
 297 Florida exposure layer used in this study is computed at a resolution of 120 arc-seconds using GDP values (in USD) from 2020.

298 Third, we use regionally calibrated impact functions (also called vulnerability functions) that relate hazard intensities to
 299 relative economic damage ratios (59) to compute event-based loss estimates. The regional calibration was conducted for nine
 300 global regions of differing socio-demographic composition and vulnerability. Here, we apply the USA-specific impact function
 301 to represent macroeconomic TC losses at the state scale; sub-county variations in structural vulnerability are not explicitly
 302 modeled, consistent with the system-level focus of this analysis. Although parameterized by wind intensity, the impact functions
 303 were calibrated to observed total TC losses and therefore capture the aggregate effects of wind, rainfall, and storm surge.

304 The resulting total loss estimates for historical TCs (1926 Great Miami Hurricane, 1992 Hurricane Andrew, 1928 Lake
 305 Okeechobee Hurricane, and 2017 Hurricane Irma; table S1) fall within the range of normalized loss estimates reported in the
 306 literature (32, Supplementary Material Table 2).

307 For the historical scenario-based insurance market stress test, we construct sequential-event scenarios by combining
 308 individual TCs: Great Miami followed by Andrew, Great Miami twice, and Irma twice. Losses are computed sequentially to
 309 account for reductions in exposed asset values after the first event. We do not model potential changes in vulnerability between
 310 events due to limited empirical evidence. These sequential scenarios should therefore be interpreted as stylized stress tests that
 311 capture exposure depletion but do not incorporate additional compounding or dynamic recovery effects. The TC hazard model
 312 uses a baseline period of 1980–2023 (30, 31), which may yield higher loss levels than industry models calibrated to longer
 313 historical records (60). Sea-level rise is not explicitly modeled, implying that long-term systemic risks may be conservatively
 314 estimated.

315 Because the insurance market operates on county-level exposure portfolios, event-based gridded losses are aggregated to
 316 county totals, which form the direct input to the financial risk propagation model (Section [Insurance market data](#)).

317 Loss estimates from the synthetic TCs are used to construct stochastic event sets spanning 10000 simulated years. From
 318 the 8800 ERA5-based and 4000 GCM-based simulated events in each TC event set, annual TC seasons are generated by
 319 sampling events with replacement according to the TC event set-specific annual frequency (Section [Tropical cyclone track
 320 data](#)). This procedure yields years without TC losses (ERA5 baseline: 28.5%), years with a single event (15.3%), and years
 321 with multiple events (56.2%). Here, “events” refers to all retained synthetic tracks passing within the 150 km Florida coastal
 322 buffer (Section [Tropical cyclone track data](#)), including storms that produce limited or spatially confined county-level losses.
 323 These synthetic year sets form the basis of the probabilistic systemic risk assessment.

324 **Wind and flood loss estimation** Because the systemic stress test requires separate accounting of wind and flood losses
 325 within the insurance market structure (Section [Layer 1: Risk absorption](#)), total TC losses must be decomposed into sub-hazard
 326 components. Explicit simulation of rainfall- and surge-driven losses using dedicated hazard models would be computationally

intensive and require additional impact-function calibration and multi-peril loss modeling, for which event-level empirical data separating wind and flood damages remain limited. Instead, we adopt a pragmatic and physically informed wind–flood attribution approach based on an external multi-hazard damage regression model. This regression-based attribution is designed for system-level probabilistic stress testing rather than event-level loss attribution.

Specifically, we partition total economic TC losses simulated in this study (Section [Hazard and loss modeling](#)) into wind and flood components using the multi-hazard regression model of Gori et al. (2025) (61, 62). That study combines county-level wind, rainfall, and storm surge intensities derived from physics-based hazard models with a regression-based damage model calibrated on observed disaster losses. Because the TC simulations in Gori et al. (2025) originate from the same underlying statistical–dynamical TC track model used here (30, 31), their hazard dataset provides a consistent basis for estimating relative wind and flood contributions.

For each TC event e and county c , we construct a compound hazard metric

$$H_{e,c} = \beta_V V_{\max,e,c} + \beta_P P_{\text{cum},e,c} + \beta_S S_{\max,e,c}, \quad (1)$$

where regression coefficients β_V , β_P , and β_S follow the regional specification of Gori et al. (2025) (61). To focus on high-intensity hazard realizations most relevant for systemic loss and insurance stress, we restrict the analysis to the upper 95th percentile of $H_{e,c}$ across all modeled events. Within this subset, we compute county-level hazard contribution ratios

$$\tilde{r}_{V,c} = \frac{\beta_V \langle V_{\max,c} \rangle_{p95}}{\beta_V \langle V_{\max,c} \rangle_{p95} + \beta_P \langle P_{\text{cum},c} \rangle_{p95} + \beta_S \langle S_{\max,c} \rangle_{p95}}. \quad (2)$$

Aggregation across Florida’s exposure-weighted counties yields a state-wide wind attribution of 84.6% (flood: 15.4%, comprising 10.2% surge and 5.2% precipitation).

For each simulated event, an event-level wind share is sampled from a Beta prior (event-specific for historical benchmark events; otherwise from a default prior centered at 84.6% wind). Total county loss is then partitioned into wind and flood components using county-specific wind shares $\tilde{r}_{V,c}$, after proportional rescaling so that the loss-weighted state-wide mean exactly equals the sampled event-level wind share. Flood loss is defined residually as the complement of wind loss.

$$L_{V,e,c} = L_{\text{total},e,c} r_{V,e,c}, \quad L_{F,e,c} = L_{\text{total},e,c} (1 - r_{V,e,c}). \quad (3)$$

Here, $r_{V,e,c}$ denotes the rescaled, event-specific county wind fraction derived from $\tilde{r}_{V,c}$.

For the historical benchmark scenarios (1926 Great Miami Hurricane, 1992 Hurricane Andrew, 1928 Lake Okeechobee Hurricane, and 2017 Hurricane Irma), the event-level prior means are set from literature-based damage reconstructions (70%, 87.5%, 30%, and 50%, respectively), with Beta priors used to represent epistemic uncertainty.

Risk propagation model

The risk propagation model translates county-level TC wind and flood losses into entity-specific financial impacts and traces how losses cascade through Florida’s residential insurance system. The model is organized into three sequential layers: (1) initial risk absorption by households, private insurers, Citizens, and the NFIP; (2) risk transfer and capital depletion via reinsurance and capital-market recoveries; and (3) public and quasi-public backstop activation (Fig. 1c). At each stage, losses are reallocated according to observed exposure shares, contractual provisions, statutory limits, and capital positions (Section [Insurance market data](#)). Across all simulations, we track household losses, insurer capital depletion and defaults, backstop activation, and system-level stress indicators (Fig. 1d).

Layer 1: Risk absorption

For each event, modeled gross wind and flood losses (Section [Wind and flood loss estimation](#)) are partitioned into insured and uninsured components. For wind losses, we calibrate the insured fraction using an empirical reconstruction approach consistent with the U.S. Billion-Dollar Disaster Database methodology (63, 64), in which total economic losses are inferred from insured losses, NFIP payments, and federal disaster assistance. Combining Florida-specific insured loss data from the Florida Office of Insurance Regulation (2017–2024) (65) with NFIP payouts (66) and federal disaster assistance (67), we estimate annual insured shares of total economic losses. To account for uncertainty in the treatment of federal disaster assistance, we compute insured shares using formulations both including and excluding public disaster aid and take the average across approaches. The resulting distribution indicates that insured shares increase with event severity and approach approximately 40% for high-loss events (Supplementary Methods). Because our stress-test scenarios focus on severe hurricane events and seasons, we represent uncertainty in the insured wind fraction using a Beta(4,6) distribution centered at 0.4. The residual share of wind losses remains with uninsured or underinsured households and does not enter the insurance system.

371 For flood losses, the insured fraction is determined using county-level NFIP take-up rates (44), accounting for participation
372 inside and outside SFHAs. Insured flood losses are capped by aggregate county coverage-in-force, and payouts are modeled on
373 a dollar-for-dollar basis up to policy limits. Residual flood losses represent uninsured household burdens.

374 Insured wind losses are allocated to private insurers and Citizens in proportion to their county-level exposure shares,
375 measured by TIV. Insured flood losses are assigned to the NFIP (Section [Insurance market data](#)). This allocation establishes
376 each entity's gross insured loss before reinsurance recoveries or capital adjustments.

377 **Sensitivity to the insured wind fraction** Sensitivity analysis indicates that the assumed insured wind fraction materially
378 affects systemic-risk outcomes. Reducing the fixed insured fraction from 0.4 to 0.1 lowers the mean FIGA residual deficit by
379 88% while increasing uninsured and underinsured household wind losses by 50% (table S4). Backstop-mechanism outcomes
380 respond more than proportionally to changes in the insured fraction because a higher insured fraction routes more wind losses
381 through insurer balance sheets, elevating default risk and amplifying downstream FIGA, Citizens, and group-capital shortfalls.
382 Because wind insurance penetration is inferred indirectly and calibrated to approximately 40% in extreme events, the model
383 may overstate coverage in smaller events but aligns with observed take-up rates in the large-loss years that dominate systemic
384 risk outcomes.

385 **Layer 2: Risk transfer and capital support**

386 **Reinsurance and catastrophe bond mechanics** Insured wind losses are partially redistributed through the FHCF, a state-run
387 public reinsurance program with entity-specific retention levels, coverage percentages, and aggregate limits. For each insurer,
388 recoverable losses are defined as insured wind losses exceeding its retention up to its contractual cap. Recoveries are computed
389 by applying the selected coverage percentage (45%, 75%, or 90%) and a 10% loss adjustment expense factor.

390 Aggregate FHCF payouts across all participating insurers are constrained by a statewide seasonal cap of USD 17 billion.
391 When modeled recoveries exceed this threshold, individual recoveries are proportionally scaled to satisfy the cap. Resulting net
392 wind losses equal insured wind losses minus FHCF recoveries.

393 An additional layer of risk transfer is provided by catastrophe bonds covering Florida wind exposure. Bonds are modeled as
394 single-occurrence, single-season layers without reinstatements. For indemnity bonds, payouts are determined by comparing
395 sponsor-specific post-FHCF net losses to attachment points and applying bond limits. For index or industry-trigger bonds,
396 payouts are based on statewide insured wind losses prior to FHCF recovery. Catastrophe bond payouts reduce insurer net losses
397 but do not modify FHCF mechanics or its seasonal cap.

398 For NFIP-insured flood losses, modeled payouts first draw on the national NFIP fund balance. Losses exceeding available
399 reserves transition to public-backstop activation in Layer 3 (Section [Layer 3: Public and quasi-public backstops](#)).

400 **Capital depletion and intragroup support** Net wind losses remaining after reinsurance and capital-market recoveries are
401 applied to each insurer's statutory surplus as regards policyholders. Insurers with negative post-loss surplus are considered
402 insolvent unless supported by an affiliated insurance group.

403 Using NAIC group identifiers, insurers are organized at the parent-group level. Group-level excess capital is defined as total
404 group surplus minus the sum of member statutory entity surpluses, floored at zero. Intragroup support is permitted only for
405 distressed statutory entities belonging to groups with a Group-to-Entity surplus ratio greater than 10, representing material
406 group-level capital buffers. Eligible distressed entities are assumed to receive capital support sufficient to restore non-negative
407 surplus, funded from available group excess capital without reducing supporting entities below zero surplus. Insurers without
408 group affiliation, or belonging to groups below the eligibility threshold, receive no support. Residual shortfalls after potential
409 group contributions determine insolvency status and transition losses to institutional stabilization mechanisms.

410 **Layer 3: Public and quasi-public backstops**

411 When private capital buffers and Layer-2 financing are exhausted, residual losses transition to statutory stabilization mechanisms
412 across three channels.

413 Insurers with negative surplus after accounting for potential intragroup support are declared insolvent. Resulting deficits are
414 transferred to the Florida Insurance Guaranty Association (FIGA), which finances policyholder claims through assessments
415 on surviving insurers subject to statutory limits (2% normal assessments and up to 4% emergency assessments of premium
416 volume). If aggregate deficits exceed FIGA's maximum assessment capacity, the remaining shortfall is recorded as residual
417 quasi-public burden, reflecting unresolved policyholder claims beyond FIGA's statutory financing capacity.

418 Citizens' net wind losses are applied to its surplus. When surplus is insufficient to absorb losses, Citizens activates its
419 statutory two-tier assessment authority. Tier 1 assessments are levied on Citizens policyholders (up to 15% of premium base),

420 followed by Tier 2 assessments on nearly all Florida property insurance policies (up to 10% of statewide premium base). Any
421 deficit remaining after both assessment tiers are exhausted represents residual public burden.

422 For NFIP-insured flood losses exceeding the national fund balance available in Layer 2, the shortfall is recorded as borrowing
423 from the U.S. Treasury under statutory backstop authority, transferring residual flood losses to the federal balance sheet.

424 **Simulation design and probabilistic assessment**

425 The risk propagation model is evaluated in two complementary settings: event-based stress tests and probabilistic seasonal
426 simulations. First, we apply the model to individual historical events and constructed sequential-event scenarios, performing
427 200 Monte Carlo iterations per event to capture parametric uncertainty while holding event characteristics fixed. Second, we
428 conduct a probabilistic assessment using 10000 synthetic TC seasons, each representing a stochastic realization of annual event
429 occurrence and associated financial parameters.

430 For each realization, county-level wind and flood losses are propagated through the deterministic financial structure
431 described above. Uncertainty arises from both variation in synthetic event realizations and parameter sampling, including
432 insured wind fractions (Beta(4,6)), wind–flood damage shares represented as Beta-distributed priors (event-specific for historical
433 benchmark events and otherwise a default prior centered at 84.6% wind; Section [Wind and flood loss estimation](#)), and stochastic
434 perturbations of total insured values (coefficient of variation 0.15). In probabilistic assessment, outcome variability is primarily
435 driven by differences in synthetic event realizations rather than parameter perturbations. We verify this with a nested Monte
436 Carlo variance decomposition: 300 seasons sampled across the loss distribution — ensuring they span the full range of
437 losses rather than being randomly drawn — are each replayed 50 times with independent parameter draws, and a one-way
438 ANOVA statistic η^2 measures the fraction of total variance attributable to between-season (hazard) differences. Hazard
439 realization explains $\geq 73\%$ of variance across all output metrics, and $\geq 95\%$ for all metrics except those linked to flooding.
440 For flood-related metrics, the remaining $\sim 25\%$ parameter contribution arises from the wind/water share Beta prior, which
441 determines how much of total damage is routed to NFIP versus private wind coverage (table S5). The propagation logic remains
442 identical across simulations.

443 **Output metrics and stress indicators**

444 Model outcomes are evaluated using metrics designed to quantify (i) loss decomposition across primary risk-absorption entities,
445 (ii) institutional stress within the insurance system, (iii) capital depletion and default dynamics, and (iv) system-level fiscal
446 impacts. Formal definitions of all metrics are provided in table S2.

447 For each event or simulated season, total economic losses are decomposed into insured wind losses (private insurers
448 and Citizens), insured flood losses (NFIP), and uninsured household losses. This decomposition characterizes the insurance
449 protection gap and the initial distribution of gross damages across households, insurers, and public or quasi-public institutions.

450 Institutional stress for public and quasi-public entities is quantified relative to their binding statutory or contractual limits
451 as implemented in the risk propagation model. For each event or simulated season, we report realized institutional stress
452 totals (FHCF reimbursements, FIGA deficits, Citizens assessment utilization, and NFIP borrowing). Within the probabilistic
453 simulations, we additionally compute annual exceedance probabilities of key capacity thresholds, including the FHCF seasonal
454 aggregate cap (USD 17 billion), FIGA's maximum assessment capacity (2% normal plus up to 4% emergency assessments of
455 surviving property insurers' written premium), Citizens' combined Tier 1 (15% of Citizens premium base) and Tier 2 (10% of
456 statewide property premium base) assessment authority, and NFIP insured losses exceeding twice its annual premium income.
457 All parameters reflect 2024 statutory conditions and are held constant across simulations.

458 Private-sector stress is measured through post-loss surplus positions after reinsurance recoveries, catastrophe bond payouts,
459 and potential intragroup capital support. We record the number of insurer insolvencies and the largest single-entity deficit.
460 These indicators capture the extent to which losses exceed available private capital buffers.

461 At the system level, we define total residual public burden as the aggregate fiscal exposure that remains after private capital
462 buffers and statutory institutional capacities are exhausted. This measure combines FHCF reimbursement shortfalls, FIGA and
463 Citizens deficits beyond assessment authority, and NFIP borrowing requirements. We compute annual exceedance probabilities
464 of total public burden relative to Florida state GDP (e.g., $> 1\%$ and $> 10\%$) and derive empirical return periods for total losses
465 and aggregate public-sector burdens across simulated year sets.

466 Empirical return periods are computed from probabilistic TC event sets by ranking outcomes in descending order, calculating
467 their cumulative exceedance frequency based on simulated event or seasonal frequencies, and defining the return period as the
468 inverse of this exceedance probability. For seasonal analyses, frequencies correspond to simulated year sets (10000 stochastic
469 seasons); for event-based analyses, they reflect the modeled annual frequency of individual storms (Section [Hazard and loss](#)

470 modeling). Seasonal and event-based return period curves coincide closely (Figure S1), so seasonal aggregation does not
 471 materially affect tail-loss frequencies.

472 Climate change and insurance market configuration experiments

473 **Future climate scenarios** Future TC projections are generated using the statistical–dynamical MIT TC model (30, 31) forced
 474 by environmental fields from CMIP6 global climate models (Section Tropical cyclone track data). We then evaluate how
 475 projected changes in TC activity translate into systemic insurance risk using a multi-model ensemble approach. Rather than
 476 using GCM-driven simulations directly to estimate future risk levels, we add climate change deltas to the ERA5 baseline. This
 477 delta approach, which is standard in the climate impact literature, avoids systematic low biases in TC intensity that arise when
 478 synthetic storms are generated from the lower-resolution environments of global climate models (31, 68).

479 For each GCM, scenario, time period, and metric, we compute the absolute climate delta as the difference between the
 480 future value and that GCM’s historical reference value (1995–2014). Deltas are aggregated across the five-GCM ensemble
 481 (median and 10th–90th percentile range) and added to the ERA5-based baseline value. Continuous metrics and empirical
 482 exceedance probabilities are treated identically: both are computed as annual means within each GCM/scenario simulation
 483 (10000 synthetic years), so the same additive scaling applies uniformly without a separate transformation. This formulation
 484 isolates the modeled climate change signal while preserving the observationally constrained baseline distribution derived from
 485 ERA5-driven simulations.

486 Uncertainty in future projections reflects both baseline sampling variability and inter-GCM spread in climate deltas. Baseline
 487 Monte Carlo uncertainty is quantified via bootstrap resampling (1000 iterations) of the 10000-year ERA5 simulations, yielding
 488 10th–90th percentile confidence intervals. Climate change uncertainty is represented by the 10th–90th percentile range of deltas
 489 across the five GCMs. These uncertainty bounds are propagated consistently to all reported future risk metrics.

490 The 2024 market architecture is held fixed across future climate scenarios, isolating the interaction between changing
 491 hazard conditions and current institutional structures without accounting for adaptation in underwriting practices, capitalization,
 492 or exposure patterns. Future stress estimates should therefore be interpreted as conditional assessments of the present-day
 493 market configuration rather than forecasts of how the market will actually evolve.

494 **Stylized market and policy interventions** We evaluate three stylized market and policy configurations representing distinct
 495 dynamics and adaptation strategies within the Florida insurance system: (i) private-market contraction (“market exit”), (ii)
 496 expanded insurance penetration and depopulation of Citizens (“penetration”), and (iii) strengthened building codes and
 497 retrofitting (“building code”). Each scenario modifies specific components of the insurance system architecture while holding all
 498 other model parameters constant throughout the 10000 simulated years, enabling isolation of intervention effects on systemic
 499 risk metrics.

500 *Private insurer market exit.* We model a private insurance market contraction that increases Citizens’ market share from 15%
 501 (baseline) to 25% of total insured value, corresponding to a 10% shift of exposure from private insurers. Of the exited private
 502 exposure, 85% transfers to Citizens and 15% becomes uninsured. Private insurers’ surplus levels are reduced in proportion to
 503 their exposure contraction, assuming partial retention of fixed capital, while Citizens’ surplus requirement scales with market
 504 share to the power of 1.2, implying an 84% increase in required surplus for a 66.7% increase in exposure. Gross wind and flood
 505 losses remain unchanged; only the pre-event allocation of exposure and capital across entities is modified. The intervention
 506 therefore redistributes financial burden without altering physical damages, increasing concentration risk within Citizens and
 507 reducing aggregate private capital buffers.

508 *Insurance penetration increase.* We model an expansion of insurance coverage and depopulation of Citizens. Wind
 509 insurance penetration increases from 40% to 60% of insurable value, and flood insurance penetration from 11% to 30%
 510 of insurable value. Flood penetration increases are implemented using county-level FEMA data distinguishing SFHA and
 511 non-SFHA areas (44). Baseline penetration rates of approximately 35% within SFHAs and 5% outside SFHAs are scaled
 512 by factors of 1.2 and 3.0, respectively, yielding an overall statewide increase from 11% to 30%. Coastal counties receive
 513 $1.5\times$ larger proportional increases than inland counties. NFIP policy counts, coverage amounts, and premium volumes are
 514 adjusted proportionally. Concurrently, Citizens’ market share decreases from 15% to 8% through active policy transfers to
 515 private insurers and higher proportional expansion of private market exposure. Insurer surplus levels scale proportionally
 516 with exposure growth. Gross wind and flood losses are unchanged; however, the insured fraction of losses increases and the
 517 uninsured household burden decreases. This intervention expands the premium base and shifts loss absorption toward the
 518 private market, while reducing Citizens’ exposure.

519 *Building code improvement.* We model structural loss reduction through enhanced building standards and retrofitting
 520 that reduce wind-related losses by 30% and flood-related losses by 25% relative to baseline vulnerability. Loss reductions

521 are applied to wind and flood loss estimates before allocation into insured and uninsured components. Exposure values and
 522 insurer capital levels remain unchanged. Unlike the previous two interventions, this scenario reduces total losses rather than
 523 reallocating them.

524 **Building code–climate offset analysis** We conduct a sensitivity analysis to determine the level of building code improvement
 525 required to offset projected mid-century climate change impacts (SSP2-4.5, 2041–2060) and maintain systemic risk levels
 526 that exist in the current climate. Using the same [Future climate scenarios](#) approach described above, we simulate historical
 527 (1995–2014) and future (2041–2060) conditions with 10000 synthetic years per model. For the future period, we evaluate 13
 528 building code levels representing combined wind and flood loss reductions ranging from 0% to 95%, with wind and flood
 529 reductions applied in a fixed 3:2 ratio.

530 For each GCM and building code level, we compute the climate delta as the difference between the mean of metric MM M
 531 across 10000 future-period simulated years (with the building-code-induced loss reduction applied) and the mean across the
 532 corresponding GCM historical reference period. Ensemble median and 10th–90th percentile deltas across the five GCMs are
 533 added to the ERA5 baseline.

534 Data availability

535 Data used in this study are available from the sources cited in the Methods section. Data from S&P Capital IQ require a
 536 commercial license and are not publicly accessible.

537 The synthetic TC data from the MIT model are proprietary and owned by WindRiskTech L.L.C., a company that provides hur-
 538 ricane risk assessments to clients worldwide. Due to proprietary restrictions, these datasets are not publicly archived. However,
 539 researchers interested in accessing the data for scientific purposes can contact WindRiskTech L.L.C. at info@windrisktech.com,
 540 subject to a non-redistribution agreement.

541 Code availability

542 For this study, we used the Python (version 3.11+) version of CLIMADA, release v6.1.0-dev (69). Source code is openly and
 543 freely available under the terms of the GNU General Public License Version 3 (55).

544 Code to reproduce the results of this paper is available at a [GitHub repository](#) (70) with the identifier 10.5281/zen-
 545 odo.19361128.

546 References

- 547 1. Swiss Re Institute, 2017: Hurricanes and the impact on the reinsurance market | Swiss Re.
 548 [https://www.swissre.com/institute/research/topics-and-risk-dialogues/climate-and-natural-catastrophe-risk/topic-](https://www.swissre.com/institute/research/topics-and-risk-dialogues/climate-and-natural-catastrophe-risk/topic-hurricanes-and-the-impact-on-the-re-insurance-market.html)
 549 [hurricanes-and-the-impact-on-the-re-insurance-market.html](https://www.swissre.com/institute/research/topics-and-risk-dialogues/climate-and-natural-catastrophe-risk/topic-hurricanes-and-the-impact-on-the-re-insurance-market.html), Accessed on 2026-02-20.
- 550 2. Seneviratne, S. I., M. G. Donat, A. J. Pitman, R. Knutti, L. J. Wilcox, and X. Zhang, 2021: Weather and climate extreme
 551 events in a changing climate. *Climate Change 2021: The Physical Science Basis. Contribution of Working Group I to the*
 552 *Sixth Assessment Report of the Intergovernmental Panel on Climate Change*, V. Masson-Delmotte, P. Zhai, A. Pirani, S. L.
 553 Connors, C. Péan, S. Berger, N. Caud, Y. Chen, L. Goldfarb, M. I. Gomis, M. Huang, K. Leitzell, E. Lonnoy, J. B. R.
 554 Matthews, T. K. Maycock, T. Waterfield, O. Yelekçi, R. Yu, and B. Zhou, Eds., Cambridge University Press, Cambridge,
 555 United Kingdom and New York, NY, USA, 1513–1766, doi:10.1017/9781009157896.014.
- 556 3. Zscheischler, J., S. Westra, B. J. Van Den Hurk, S. I. Seneviratne, P. J. Ward, A. Pitman, A. Aghakouchak, D. N. Bresch,
 557 M. Leonard, T. Wahl, and X. Zhang, 2018: Future climate risk from compound events. *Nature Climate Change*, **8** (6),
 558 469–477, doi:10.1038/s41558-018-0156-3.
- 559 4. Kousky, C., 2019: The Role of Natural Disaster Insurance in Recovery and Risk Reduction. doi:10.1146/
 560 annurev-resource-100518-094028.
- 561 5. IPCC, 2023: *Climate Change 2023: Synthesis Report. Contribution of Working Groups I, II and III to the Sixth As-*
 562 *essment Report of the Intergovernmental Panel on Climate Change*. IPCC, Geneva, Switzerland, doi:10.59327/IPCC/
 563 AR6-9789291691647.
- 564 6. UNDRR, 2022: *Global Assessment Report on Disaster Risk Reduction 2022: Our World at Risk: Transforming Governance*
 565 *for a Resilient Future*. United Nations Office for Disaster Risk Reduction, Geneva, Switzerland.
- 566 7. Gallagher, J., and D. Hartley, 2017: Household Finance after a Natural Disaster: The Case of Hurricane Katrina. *American*
 567 *Economic Journal: Economic Policy*, **9** (3), 199–228, doi:10.1257/pol.20140273.
- 568 8. Kunreuther, H., and M. Useem, Eds., 2010: *Learning from Catastrophes: Strategies for Reaction and Response*. Pearson P
 569 T R, Upper Saddle River, N.J.

- 570 **9.** Jarzabkowski, P., K. Chalkias, E. Cacciatori, and R. Bednarek, 2023: *Disaster Insurance Reimagined: Protection in a Time*
571 *of Increasing Risk*. 1st ed., Oxford University Press Oxford, doi:10.1093/oso/9780192865168.001.0001.
- 572 **10.** Kousky, C., G. Treuer, and K. J. Mach, 2024: Insurance and climate risks: Policy lessons from three bounding scenarios.
573 *Proceedings of the National Academy of Sciences*, **121** (48), e2317875 121, doi:10.1073/pnas.2317875121.
- 574 **11.** Pielke, R. A., J. Gratz, C. W. Landsea, D. Collins, M. A. Saunders, and R. Musulin, 2008: Normalized Hurricane Damage
575 in the United States: 1900–2005. *Natural Hazards Review*, **9** (1), 29–42, doi:10.1061/(ASCE)1527-6988(2008)9:1(29).
- 576 **12.** Kousky, C., 2022: *Understanding Disaster Insurance: New Tools for a More Resilient Future*. Island Press, Washington.
- 577 **13.** California Department of Insurance, 2024: 2024 annual report of the insurance commissioner. Tech. rep., California
578 Department of Insurance, Sacramento, CA, USA.
- 579 **14.** Gray, I., 2021: Hazardous simulations: Pricing climate risk in US coastal insurance markets. *Economy and Society*, **50** (2),
580 196–223, doi:10.1080/03085147.2020.1853358.
- 581 **15.** Kousky, C., and L. Medders, 2024: The evolution of florida’s public-private approach to property insurance. Report, Florida
582 Policy Project.
- 583 **16.** Hemmati, M., I. P. Gray, and S. G. Bowen, 2025: The growing void in the U.S. homeowners insurance market: Who should
584 bear the rising cost of climate change? *npj Climate Action*, **4** (1), 1–7, doi:10.1038/s44168-025-00231-8.
- 585 **17.** Basel Committee on Banking Supervision, 2011: *Basel III: A Global Regulatory Framework for More Resilient Banks and*
586 *Banking Systems*. December 2010 (rev. june 2011) ed., Basel Bank for International Settlements 2011.
- 587 **18.** International Monetary Fund (IMF), 2012: Macrofinancial stress testing—principles and practices. Tech. rep., International
588 Monetary Fund.
- 589 **19.** Board of Governors of the Federal Reserve System, 2022: Stress tests and capital planning.
590 <https://www.federalreserve.gov/supervisionreg/stress-tests-capital-planning.htm>, Accessed on 2026-03-31.
- 591 **20.** Battiston, S., A. Mandel, I. Monasterolo, F. Schütze, and G. Visentin, 2017: A climate stress-test of the financial system.
592 *Nature Climate Change*, **7** (4), 283–288, doi:10.1038/nclimate3255.
- 593 **21.** Network for Greening the Financial System (NGFS), 2024: NGFS climate scenarios for central banks and supervisors—
594 phase V. Tech. rep., Network for Greening the Financial System (NGFS).
- 595 **22.** Dunz, N., T. Emambakhsh, T. Hennig, M. Kaijser, C. Kouratzoglou, and C. Salleo, 2021: ECB’s Economy-Wide Climate
596 Stress Test. *SSRN Electronic Journal*, doi:10.2139/ssrn.3929178.
- 597 **23.** Swiss Re Institute, 2024: Sigma 1/2024: Natural catastrophes in 2023: Gearing up for today’s and tomorrow’s weather
598 risks.
- 599 **24.** Task Force on Climate-related Financial Disclosures, 2017: Final report: Recommendations of the task force on climate-
600 related financial disclosures. Technical report, Financial Stability Board.
- 601 **25.** National Association of Insurance Commissioners (NAIC), 2026: NAIC climate risk disclosure survey.
602 <https://www.insurance.ca.gov/0250-insurers/0300-insurers/0100-applications/ClimateSurvey/index.cfm>, Accessed on 2026-
603 03-31.
- 604 **26.** European Insurance and Occupational Pensions Authority (EIOPA), 2022: Methodological principles of insurance stress
605 testing—climate change component. Tech. rep., European Insurance and Occupational Pensions Authority (EIOPA).
- 606 **27.** Abrahams, D., and T. Robustelli, 2025: Climate Change, Housing, and Homeowners Insurance in Florida: Lessons
607 for California. <http://newamerica.org/future-land-housing/briefs/insurance-in-florida-lessons-for-california/>, Accessed on
608 2026-01-28.
- 609 **28.** Kaufmann, L., 2024: Florida’s Home Insurance Industry May Be Worse Than Anyone Realizes. Accessed on 2026-01-28.
- 610 **29.** Knapp, K. R., M. C. Kruk, D. H. Levinson, H. J. Diamond, and C. J. Neumann, 2010: The International Best Track
611 Archive for Climate Stewardship (IBTrACS). *Bulletin of the American Meteorological Society*, **91** (3), 363–376, doi:
612 10.1175/2009BAMS2755.1.
- 613 **30.** Emanuel, K., S. Ravela, E. Vivant, and C. Risi, 2006: A Statistical Deterministic Approach to Hurricane Risk Assessment.
614 *Bulletin of the American Meteorological Society*, **87** (3), S1–S5, doi:10.1175/bams-87-3-emanuel.
- 615 **31.** Emanuel, K., R. Sundararajan, and J. Williams, 2008: Hurricanes and global warming: Results from downscaling IPCC
616 AR4 simulations. *Bulletin of the American Meteorological Society*, **89** (3), 347–367, doi:10.1175/BAMS-89-3-347.
- 617 **32.** Muller, J., K. Mooney, S. G. Bowen, P. J. Klotzbach, T. Martin, T. J. Philp, B. Dhruvkumar, R. S. Dixon, and S. B. Girimu-
618 rugan, 2025: Normalized Hurricane Damage in the United States: 1900–2022. *Bulletin of the American Meteorological*
619 *Society*, **106** (1), E51–E67, doi:10.1175/BAMS-D-23-0280.1.
- 620 **33.** Wolf, D., and K. Takeuchi, 2025: Are Building Codes an Effective Adaptation to Wind Risk? Evidence from Remotely
621 Detected Blue Tarps.
- 622 **34.** Insurance Institute for Business & Home Safety, 2025: 2025 FORTIFIED home standards. Accessed on 2026-02-19.
- 623 **35.** Alabama Department of Insurance and Center for Risk and Insurance Research, 2025: Performance of IBHS FORTIFIED
624 Home™ construction in hurricane sally. Accessed on 2026-02-19.

- 625 **36.** Meiler, S., A. Ciullo, C. M. Kropf, K. Emanuel, and D. N. Bresch, 2023: Uncertainties and sensitivities in the quantification
626 of future tropical cyclone risk. *Communications Earth & Environment*, **4** (1), 1–10, doi:10.1038/s43247-023-00998-w.
- 627 **37.** Abatzoglou, J. T., and A. P. Williams, 2016: Impact of anthropogenic climate change on wildfire across western US forests.
628 *Proceedings of the National Academy of Sciences*, **113** (42), 11 770–11 775, doi:10.1073/pnas.1607171113.
- 629 **38.** Mishra, A., A. Arun, E. Kodra, E. Smull, O. Woolcock, T. Doe, J. Marlowe, and A. R. Ganguly, 2026: Physical
630 climate risk creates challenges and opportunities in US municipal finance. *Nature Cities*, **3** (1), 11–21, doi:10.1038/
631 s44284-025-00365-0.
- 632 **39.** Amornsiripanitch, N., S. Biswas, J. Orellana-Li, and D. Zink, 2025: Measuring flood underinsurance in the USA. *Nature*
633 *Climate Change*, 1–7, doi:10.1038/s41558-025-02396-w.
- 634 **40.** Florida Hurricane Catastrophe Fund, 2024: Florida hurricane catastrophe fund 2024 annual report. State Board of
635 Administration of Florida, Accessed on 2026-03-19.
- 636 **41.** Florida Office of Insurance Regulation, 2024: Quarterly Residential Market Share Reports. [https://fior.gov/tools-and-](https://fior.gov/tools-and-data/residential-market-share-reports)
637 [data/residential-market-share-reports](https://fior.gov/tools-and-data/residential-market-share-reports), Accessed on 2026-03-19.
- 638 **42.** Citizens Property Insurance Corporation, 2024: Policies in force. <https://www.citizensfla.com/policies-in-force>, Accessed
639 on 2026-03-31.
- 640 **43.** Federal Emergency Management Agency (FEMA), 2024: FIMA NFIP redacted policies (v2). U.S. Department of Homeland
641 Security, <https://www.fema.gov/openfema-data-page/fima-nfip-redacted-policies-v2>, Accessed on 2026-03-19.
- 642 **44.** Federal Emergency Management Agency (FEMA), 2025: OpenFEMA dataset: NFIP residential penetration rates – v1.
643 U.S. Department of Homeland Security, <https://www.fema.gov/openfema-data-page/nfip-residential-penetration-rates-v1>,
644 Accessed on 2026-03-19.
- 645 **45.** Citizens Property Insurance Corporation, 2024: Annual statement of the citizens property insurance corporation for the
646 year ended december 31, 2024. Tech. rep., Citizens Property Insurance Corporation, Tallahassee, FL.
- 647 **46.** Congressional Research Service, 2025: National flood insurance program borrowing authority.
648 https://www.congress.gov/crs_external_products/IN/PDF/IN10784/IN10784.43.pdf, Accessed on 2026-03-31.
- 649 **47.** State Board of Administration of Florida, and Florida Hurricane Catastrophe Fund, 2023: Florida hurricane catastrophe
650 fund: 2023 annual report. Tech. rep., State Board of Administration of Florida, Tallahassee, FL.
- 651 **48.** Artemis.bm, 2024: Catastrophe bond and insurance-linked securities deal directory. <https://www.artemis.bm/deal-directory/>,
652 Accessed on 2026-03-31.
- 653 **49.** Hersbach, H., B. Bell, P. Berrisford, S. Hirahara, A. Horányi, J. Muñoz-Sabater, J. Nicolas, C. Peubey, R. Radu, D. Schepers,
654 A. Simmons, C. Soci, S. Abdalla, X. Abellan, G. Balsamo, P. Bechtold, G. Biavati, J. Bidlot, M. Bonavita, G. De Chiara,
655 P. Dahlgren, D. Dee, M. Diamantakis, R. Dragani, J. Flemming, R. Forbes, M. Fuentes, A. Geer, L. Haimberger,
656 S. Healy, R. J. Hogan, E. Hólm, M. Janisková, S. Keeley, P. Laloyaux, P. Lopez, C. Lupu, G. Radnoti, P. de Rosnay,
657 I. Rozum, F. Vamborg, S. Villaume, and J.-N. Thépaut, 2020: The ERA5 global reanalysis. *Quarterly Journal of the Royal*
658 *Meteorological Society*, **146** (730), 1999–2049, doi:10.1002/qj.3803.
- 659 **50.** Swart, N. C., J. N. S. Cole, V. V. Kharin, M. Lazare, J. F. Scinocca, N. P. Gillett, J. Anstey, V. Arora, J. R. Christian,
660 S. Hanna, Y. Jiao, W. G. Lee, F. Majaess, O. A. Saenko, C. Seiler, C. Seinen, A. Shao, M. Sigmond, L. Solheim, K. von
661 Salzen, D. Yang, and B. Winter, 2019: The Canadian Earth System Model version 5 (CanESM5.0.3). *Geoscientific Model*
662 *Development*, **12** (11), 4823–4873, doi:10.5194/gmd-12-4823-2019.
- 663 **51.** Voldoire, A., D. Saint-Martin, S. Sénési, B. Decharme, A. Alias, M. Chevallier, J. Colin, J.-F. Guérémy, M. Michou,
664 M.-P. Moine, P. Nabat, R. Roehrig, D. Salas y Mélia, R. Sférian, S. Valcke, I. Beau, S. Belamari, S. Berthet, C. Cassou,
665 J. Cattiaux, J. Deshayes, H. Douville, C. Ethé, L. Franchistéguy, O. Geoffroy, C. Lévy, G. Madec, Y. Meurdesoif,
666 R. Msadek, A. Ribes, E. Sanchez-Gomez, L. Terray, and R. Waldman, 2019: Evaluation of CMIP6 DECK Experiments
667 With CNRM-CM6-1. *Journal of Advances in Modeling Earth Systems*, **11** (7), 2177–2213, doi:10.1029/2019MS001683.
- 668 **52.** EC Earth Consortium, 2019: EC-Earth-Consortium EC-Earth3 model output prepared for CMIP6 ScenarioMIP ssp245.
669 Accessed on 2023-02-16, doi:10.22033/ESGF/CMIP6.4880.
- 670 **53.** Hourdin, F., C. Rio, J.-Y. Grandpeix, J.-B. Madeleine, F. Cheruy, N. Rochetin, A. Jam, I. Musat, A. Idelkadi, L. Fairhead,
671 M.-A. Foujols, L. Mellul, A.-K. Traore, J.-L. Dufresne, O. Boucher, M.-P. Lefebvre, E. Millour, E. Vignon, J. Jouhaud, F. B.
672 Diallo, F. Lott, G. Gastineau, A. Caubel, Y. Meurdesoif, and J. Ghattas, 2020: LMDZ6A: The Atmospheric Component of
673 the IPSL Climate Model With Improved and Better Tuned Physics. *Journal of Advances in Modeling Earth Systems*, **12** (7),
674 e2019MS001 892, doi:10.1029/2019MS001892.
- 675 **54.** Tatebe, H., T. Ogura, T. Nitta, Y. Komuro, K. Ogochi, T. Takemura, K. Sudo, M. Sekiguchi, M. Abe, F. Saito, M. Chikira,
676 S. Watanabe, M. Mori, N. Hirota, Y. Kawatani, T. Mochizuki, K. Yoshimura, K. Takata, R. O’ishi, D. Yamazaki, T. Suzuki,
677 M. Kurogi, T. Kataoka, M. Watanabe, and M. Kimoto, 2019: Description and basic evaluation of simulated mean
678 state, internal variability, and climate sensitivity in MIROC6. *Geoscientific Model Development*, **12** (7), 2727–2765,
679 doi:10.5194/gmd-12-2727-2019.

55. Aznar-Siguan, G., and D. N. Bresch, 2019: CLIMADA v1: A global weather and climate risk assessment platform. *Geoscientific Model Development*, **12** (7), 3085–3097, doi:10.5194/gmd-12-3085-2019.
56. IPCC, 2012: *Managing the Risks of Extreme Events and Disasters to Advance Climate Change Adaptation. A Special Report of Working Groups I and II of the Intergovernmental Panel on Climate Change* [Field, C.B., V. Barros, T.F. Stocker, D. Qin, D.J. Dokken, K.L. Ebi, M.D. doi:10.1017/CBO9781139177245.
57. Holland, G., 2008: A revised hurricane pressure-wind model. *Monthly Weather Review*, **136** (9), 3432–3445, doi:10.1175/2008MWR2395.1.
58. Eberenz, S., D. Stocker, T. Rössli, and D. N. Bresch, 2020: Asset exposure data for global physical risk assessment. *Earth System Science Data*, **12** (2), 817–833, doi:10.5194/essd-12-817-2020.
59. Eberenz, S., S. Lüthi, and D. N. Bresch, 2021: Regional tropical cyclone impact functions for globally consistent risk assessments. *Natural Hazards and Earth System Sciences*, **21** (1), 393–415, doi:10.5194/nhess-21-393-2021.
60. Gibson, M., and B. Hohermuth, 2025: Climate risk and insurance-linked securities: Navigating a shifting landscape. <https://www.schroders.com/en-us/us/non-resident-clients/insights/climate-risk-and-insurance-linked-securities-navigating-a-shifting-landscape/>, Accessed on 2026-02-24.
61. Gori, A., N. Lin, D. Chavas, M. Oppenheimer, and S. Xian, 2025: Sensitivity of tropical cyclone risk across the US to changes in storm climatology and socioeconomic growth. *Environmental Research Letters*, **20** (6), 064050, doi:10.1088/1748-9326/add60d.
62. Gori, A., 2025: Tropical Cyclone Synthetic Hazard and Damage Simulations. DesignSafe-CI, Accessed on 2026-02-12, doi:10.17603/ds2-0jkm-h487.
63. Smith, A. B., and R. W. Katz, 2013: US billion-dollar weather and climate disasters: Data sources, trends, accuracy and biases. *Natural Hazards*, **67** (2), 387–410, doi:10.1007/s11069-013-0566-5.
64. Smith, A. B., and J. L. Matthews, 2015: Quantifying uncertainty and variable sensitivity within the US billion-dollar weather and climate disaster cost estimates. *Natural Hazards*, **77** (3), 1829–1851, doi:10.1007/s11069-015-1678-x.
65. Florida Office of Insurance Regulation, 2026: Catastrophe Reporting. <https://floir.gov/tools-and-data/catastrophe-reporting>, Accessed on 2026-03-19.
66. National Flood Insurance Program, 2026: Historical NFIP Claims Information and Trends. <https://www.floodsmart.gov/historical-nfip-claims-information-and-trends>, Accessed on 2026-03-19.
67. Federal Emergency Management Agency (FEMA), 2026: Disaster Declarations Summaries - v2. U.S. Department of Homeland Security, <https://www.fema.gov/openfema-data-page/disaster-declarations-summaries-v2>, Accessed on 2026-03-19.
68. Camargo, S. J., 2013: Global and regional aspects of tropical cyclone activity in the CMIP5 models. *Journal of Climate*, **26** (24), 9880–9902, doi:10.1175/JCLI-D-12-00549.1.
69. Siguan, G. A., D. N. Bresch, S. Eberenz, J. Hartman, M. Perus, T. Rössli, D. Stocker, V. Bozzini, C. B. Steinmann, E. Mühlhofer, R. Bungerer, I. J. Sauer, S. Lüthi, P. M. M. Kam, S. Meiler, A. Ciullo, T. Vogt, B. P. Guillod, C. M. Kropf, E. Schmid, C. Fairless, J. Wüthrich, Z. Stalhandske, Y. Yu, L. Riedel, R. Portmann, N. Colombi, L. Villiger, T. Schmid, L. Severino, S. Juhel, V. Gebhart, and D. Araya, 2025: CLIMADA Core Python Package. Zenodo, Accessed on 2026-03-23, doi:10.5281/zenodo.17233409.
70. Meiler, S., 2026: Simanameiler/systemic_insurance_risk_fl_pub: V1.0.0. Zenodo, Accessed on 2026-03-31, doi:10.5281/zenodo.19361128.
71. US Bureau of Labor Statistics, 2026: Consumer Price Index for All Urban Consumers (CPI-U). <https://data.bls.gov/PDQWeb/cu>, Accessed on 2026-03-19.

721 Acknowledgements

722 Funding

723 SM acknowledges support from the Swiss National Science Foundation Postdoc.Mobility Fellowship (P500PN_222189) and
724 from the Stanford Urban Resilience Initiative. NSD acknowledges support from Stanford University.

725 The development of the risk propagation model underlying this study was initiated in collaboration with the Insurance Policy
726 Advisory Committee (IPAC) of the U.S. Federal Reserve System, for which Simona Meiler developed an initial flow-of-risk
727 modeling approach. We thank members of the IPAC Property Insurance Working Group for valuable discussions and insights
728 that informed the conceptual design of the model. The analysis presented here represents independent academic work and does
729 not reflect the views of the Federal Reserve System or its committees.

730 **Author contributions statement**

731 Conceptualization: SM, SIJ

732 Methodology: SM

733 Visualization: SM

734 Datasets: SM, SIJ, KE

735 Writing - original draft: SM

736 Writing - review & editing: SM, SIJ, KE, NSD, JWB

737 **Competing interests**

738 All authors (SM, SIJ, KE, NSD, JWB) declare no competing interests. Kerry Emanuel is on the board of Trusted Resource
739 Underwriters, which insures homeowners in Florida.

Supplementary Information for article "Stress testing insurance market stability under climate risk"

Supplementary Methods

Estimation of insured loss fractions for tropical cyclone events

To estimate the fraction of economic losses covered by insurance for tropical cyclone events, we reconstruct empirical relationships between insured and total economic losses using Florida-specific data. Our approach follows the methodology of the U.S. Billion-Dollar Weather and Climate Disaster Database (63, 64), in which total economic losses are inferred from insured losses, National Flood Insurance Program (NFIP) payouts, and federal disaster assistance.

Total economic losses are estimated as:

$$L_{\text{econ}} = 2 \cdot L_{\text{insured}} + L_{\text{NFIP}} + L_{\text{FDA}}, \quad (4)$$

where L_{insured} denotes insured losses reported by the Florida Office of Insurance Regulation (OIR), L_{NFIP} represents NFIP payouts, and L_{FDA} denotes federal disaster assistance. Following (63), the factor of two applied to insured losses accounts for uninsured private losses.

Because the treatment of federal disaster assistance in economic loss accounting is uncertain, we compute two estimates of economic losses: one including L_{FDA} and one excluding it. The insured fraction is then calculated for both formulations as:

$$f_{\text{insured}} = \frac{L_{\text{insured}}}{L_{\text{econ}}}, \quad (5)$$

and averaged across both estimates.

We compile insured loss data from the Florida OIR for hurricane-related losses (2017–2020 and 2022–2024) (65), complemented by NFIP payout data from FEMA's Floodsmart database (66) and federal disaster assistance from FEMA disaster summaries (67). All monetary values are converted to 2024 USD using the Consumer Price Index (CPI-U) from the U.S. Bureau of Labor Statistics (71).

Estimated insured shares vary substantially across years (table S1), ranging from approximately 10% in low-loss years to nearly 50% in high-loss years. Years with large economic losses (exceeding \$25 billion) consistently exhibit insured shares above 40%, indicating that insurance penetration increases with event severity.

Table S1: Insured and estimated economic losses and resulting insured shares for Florida hurricane events (2017–2024).

Economic losses are estimated using formulations including and excluding federal disaster assistance (FDA). All values are converted to 2024 USD.

Year	Insured losses	Est econ loss (incl. FDA)	f_{insured} (incl.)	Est econ loss (excl. FDA)	f_{insured} (excl.)
2017	28,159,458,046	60,750,223,673	46.35%	57,644,860,280	48.85%
2018	11,472,501,417	26,081,530,262	43.99%	23,251,364,093	49.34%
2019	23,342,615	198,468,914	11.76%	80,793,892	28.89%
2020	699,057,474	2,041,794,621	34.24%	1,783,712,209	39.19%
2021	—	—	—	—	—
2022	23,914,182,689	56,175,193,964	42.57%	53,075,926,756	45.06%
2023	318,470,377	1,754,055,340	18.16%	1,315,565,662	24.21%
2024	7,466,073,319	25,060,543,556	29.79%	22,700,454,161	32.89%
Mean			32.41%		38.35%
Median			34.24%		39.19%
High-loss mean (> \$25B)			40.68%		44.03%

Averaging across all years, estimation approaches, and subsets of high-loss years yields an overall mean insured share of 38.9%. Given that the stress-test scenarios considered in this study focus on severe hurricane events and loss years, we adopt a representative insured fraction of 40% for wind-related losses. To account for uncertainty, this fraction is implemented as a Beta distribution centered at 0.4 (Beta(4,6)), reflecting variability around the empirical mean while emphasizing higher insured shares in large-loss events.

Table S2: Definitions of systemic risk metrics used in the main text and Supplementary Information.

Metric	Unit	Definition	Used in
<i>Loss decomposition</i>			
Total loss	USD	Aggregate economic tropical cyclone loss before redistribution across insurance and public backstop layers.	Table 1, Tables S2–S3, Figs. 2, 6
Insured wind – private	USD	Wind-related losses allocated to private admitted-market insurers in the initial risk-absorption layer.	Table 1, Tables S2–S3, Fig. 2
Citizens wind	USD	Wind-related losses allocated to Citizens in the initial risk-absorption layer.	Table 1, Tables S2–S3, Fig. 2
Insured flood – NFIP	USD	Flood-related losses allocated to the NFIP.	Table 1, Tables S2–S3, Fig. 2
Un/underinsured wind	USD	Wind-related damages not covered by private insurance or Citizens because of un- or underinsurance.	Table 1, Tables S2–S3, Fig. 2
Un/underinsured flood	USD	Flood-related damages not covered by the NFIP because of un- or underinsurance.	Table 1, Tables S2–S3, Fig. 2
Household burden	USD	Combined un/underinsured wind and flood losses.	Table 1, Tables S2–S3, Fig. 2
Insured / un/insured share	%	Share of total loss that is insured or un/underinsured.	Fig. 2
<i>Institutional stress and public burden</i>			
FHCF shortfall	USD	Unrecovered wind losses resulting when the FHCF season-wide payout cap binds.	Table 1, Tables S2–S3, Figs. 2, S2
FIGA residual	USD	Residual deficit remaining after insurer insolvencies are absorbed through the FIGA, subject to its assessment limits.	Table 1, Tables S2–S3, Figs. 2, S2
Citizens deficit	USD	Residual deficit remaining after Citizens' surplus and assessment capacity are exhausted.	Table 1, Tables S2–S3, Figs. 2, S2
NFIP Treasury borrowing	USD	Portion of Florida-attributable NFIP losses financed through borrowing from the U.S. Treasury once NFIP fund balances are insufficient.	Table 1, Tables S2–S3, Figs. 2, S2
Total public burden	USD	The sum of FHCF shortfall, FIGA residual, Citizens deficit, and NFIP Treasury borrowing.	Table 1, Tables S2–S3, Figs. 2, 6
<i>Capital depletion and default outcomes</i>			
Private defaults	#	Number of private insurer entities that become insolvent under a simulated event or season after modeled capital depletion.	Table S2, Figs. 3–4, S2
Largest single-entity deficit	USD	Maximum capital shortfall of any one insurer entity in a simulated event or season.	Table S2, Figs. 3–4, Fig. S2
<i>Stress ratios</i>			
FHCF utilization factor	ratio	Share of the FHCF season-wide statutory payout capacity utilized in a given scenario or simulation. A value of 1 indicates that the cap is fully used.	Table S2
Citizens assessment stress factor	ratio	Citizens' deficit divided by its maximum assessment capacity (Tier 1 + Tier 2). Values above 1 indicate that the funding need exceeds statutory capacity.	Table S2
FIGA stress factor	ratio	Insolvency-related deficit relative to FIGA's effective maximum assessment capacity. Values above 1 indicate exceedance of capacity.	Table S2
NFIP Florida stress factor	ratio	Florida-attributable NFIP claims paid divided by Florida NFIP annual premium volume.	Table S2
<i>Probabilistic exceedance metrics</i>			
Defaults > 10	annual probability (%)	Probability that more than ten private insurers default in a simulated tropical cyclone season.	Figs. 3–5, Table S4
Single deficit > \$1B	annual probability (%)	Probability that the largest single-company deficit exceeds USD 1 billion in a simulated season.	Figs. 3–5, Table S4
FHCF > 100% cap	annual probability (%)	Probability that modeled FHCF payouts reach or exceed the season-wide statutory cap.	Figs. 3–5, Table S4
FIGA > 100% capacity	annual probability (%)	Probability that FIGA funding needs exceed its statutory assessment capacity.	Figs. 3–5, Table S4
Citizens > 100% capacity	annual probability (%)	Probability that Citizens' deficit exceeds its assessment capacity.	Figs. 3–5, Table S4
NFIP > 200% annual premium	annual probability (%)	Probability that Florida-attributable NFIP losses exceed twice Florida NFIP annual premium income.	Figs. 3–5, Table S4
Public burden > 1% Florida GDP	annual probability (%)	Probability that total public burden exceeds 1% of Florida's GDP in a simulated season.	Figs. 3–5, Table S4
Public burden > 10% Florida GDP	annual probability (%)	Probability that total public burden exceeds 10% of Florida's GDP in a simulated season.	Figs. 3–5, Table S4

Table S3: Scenario-based loss decomposition and institutional stress outcomes for Florida hurricane events. Results are reported as mean values across stochastic realizations, with uncertainty ranges in parentheses indicating the 5th–95th percentiles. Metric definitions are provided in table S2.

Metric	Great Miami	Andrew	Lake Okechobee	Irma	Great Miami then Andrew	Double Great Miami	Double Irma
<i>Loss decomposition</i>							
Total loss (USD)	170.4B (170.4-170.4B)	114.2B (114.2-114.2B)	156.9B (156.9-156.9B)	32.0B (32.0-32.0B)	266.5B (266.5-266.5B)	321.1B (321.1-321.1B)	62.4B (62.4-62.4B)
Insured wind – private (USD)	36.9B (20.2-56.1B)	29.0B (14.0-46.4B)	16.3B (4.3-31.6B)	6.0B (2.8-9.5B)	61.4B (35.6-90.6B)	69.3B (42.7-98.1B)	11.5B (7.4-15.9B)
Citizens wind (USD)	10.3B (4.9-17.1B)	10.3B (4.6-17.7B)	2.6B (0.7-5.1B)	0.5B (0.2-0.7B)	18.8B (9.7-30.0B)	19.4B (10.5-30.5B)	0.9B (0.6-1.2B)
Insured flood – NFIP (USD)	15.0B (4.9-27.7B)	4.9B (0.5-12.9B)	17.0B (10.5-22.4B)	2.6B (1.3-4.0B)	19.8B (9.4-31.9B)	28.1B (16.1-41.4B)	5.2B (3.6-6.7B)
Un/Underinsured wind (USD)	72.2B (42.5-101.3B)	60.5B (37.8-84.5B)	28.3B (7.6-55.4B)	9.7B (4.7-14.9B)	122.9B (84.4-165.0B)	136.7B (96.0-180.5B)	18.7B (12.8-25.5B)
Un/Underinsured flood (USD)	35.9B (11.4-66.8B)	9.4B (0.9-24.7B)	92.6B (57.3-121.9B)	13.3B (6.5-20.1B)	43.7B (20.5-70.7B)	67.7B (38.5-100.1B)	26.1B (18.0-33.8B)
<i>Institutional stress</i>							
Total public burden (USD)	26.1B (15.4-38.8B)	11.7B (4.1-22.3B)	18.4B (16.6-20.9B)	0.2B (0.0-0.8B)	51.0B (28.7-74.0B)	65.4B (42.7-88.3B)	3.1B (2.1-4.0B)
FHCF shortfall (USD)	1.7B (0.0-8.0B)	0.0B (0.0-0.0B)	0.0B (0.0-0.0B)	0.0B (0.0-0.0B)	5.6B (0.0-11.6B)	8.0B (0.0-12.7B)	0.0B (0.0-0.0B)
FIGA residual (USD)	7.0B (3.2-13.4B)	4.2B (1.1-10.0B)	3.3B (0.0-8.8B)	0.1B (0.0-0.7B)	15.8B (6.2-27.7B)	19.1B (8.5-31.1B)	1.3B (0.1-2.8B)
Citizens deficit (USD)	5.8B (3.1-11.4B)	5.2B (1.9-11.9B)	1.6B (0.0-4.0B)	0.0B (0.0-0.0B)	13.2B (4.7-24.1B)	13.6B (5.5-24.7B)	0.0B (0.0-0.3B)
NFIP treasury borrowing (USD)	11.5B (1.4-24.3B)	2.2B (0.0-9.4B)	13.6B (7.1-18.9B)	0.1B (0.0-0.5B)	16.4B (6.0-28.5B)	24.7B (12.7-38.0B)	1.8B (0.2-3.3B)
<i>Capital & default assessment</i>							
Private defaults (#)	18 (15-22)	16 (12-20)	13 (0-18)	5 (0-11)	21 (18-23)	22 (19-24)	12 (8-14)
Largest single-entity deficit (USD)	1.9B (1.1-3.3B)	1.2B (0.4-2.8B)	1.0B (0.0-2.4B)	0.1B (0.0-0.4B)	3.8B (1.6-6.8B)	4.6B (2.2-7.5B)	0.6B (0.2-1.0B)
<i>Stress ratios</i>							
FHCF utilization factor	0.79 (0.20-1.00)	0.74 (0.25-0.93)	0.02 (0.00-0.08)	0.00 (0.00-0.00)	0.98 (0.87-1.00)	0.98 (0.92-1.00)	0.00 (0.00-0.01)
Citizens assessment stress factor	6.46 (3.43-12.64)	5.83 (2.16-13.26)	1.74 (0.00-4.46)	0.00 (0.00-0.00)	14.67 (5.26-26.77)	15.13 (6.07-27.40)	0.06 (0.00-0.29)
FIGA stress factor	0.95 (0.91-0.98)	0.88 (0.74-0.97)	0.77 (0.00-0.97)	0.17 (0.00-0.67)	0.98 (0.95-0.99)	0.98 (0.97-0.99)	0.70 (0.23-0.89)
NFIP Florida stress factor	10.73 (3.49-19.86)	3.54 (0.35-9.23)	12.19 (7.56-16.02)	1.90 (0.95-2.85)	14.20 (6.74-22.89)	20.13 (11.54-29.68)	3.71 (2.58-4.79)

Table S4: Loss decomposition and public institutional burden across climate and policy scenarios. Values show expected annual losses and institutional burdens under present-day baseline conditions, future climate scenarios (2050 and 2100 under SSP2-4.5 and SSP5-8.5), and illustrative market and policy interventions evaluated under present-day climate forcing. Values are reported as means in billion USD with uncertainty ranges (10th–90th percentile) in parentheses.

Metric (USD B)	Baseline	2050 SSP2-4.5	2050 SSP5-8.5	2100 SSP2-4.5	2100 SSP5-8.5	Market Exit	Insurance Penetration	Building Codes
<i>Loss decomposition</i>								
Total loss	19.3 (0.0–37.8)	31.5 (15.3–45.5)	34.9 (17.6–55.6)	41.9 (18.3–50.0)	59.2 (22.2–104.2)	19.3 (0.0–37.8)	19.3 (0.0–37.9)	19.3 (0.0–38.0)
Insured wind – private	5.5 (0.0–11.6)	13.9 (6.7–19.9)	15.4 (7.8–24.3)	18.5 (8.1–22.1)	26.2 (9.8–46.0)	4.7 (0.0–9.8)	8.1 (0.0–17.3)	3.8 (0.0–8.1)
Citizens wind	1.1 (0.0–1.8)	2.6 (1.3–3.8)	2.9 (1.5–4.6)	3.4 (1.5–4.1)	4.7 (1.8–8.6)	1.9 (0.0–3.5)	1.7 (0.0–2.8)	0.8 (0.0–1.2)
Insured flood – NFIP	0.6 (0.0–0.9)	1.5 (0.8–2.3)	1.7 (0.8–2.7)	1.9 (0.9–2.3)	2.7 (1.0–5.0)	0.6 (0.0–0.9)	1.7 (0.0–2.4)	0.5 (0.0–0.7)
Un/underinsured wind	9.7 (0.0–19.8)	7.3 (3.6–10.8)	8.3 (4.1–13.1)	9.9 (4.3–11.8)	14.0 (5.2–24.5)	9.7 (0.0–19.8)	6.5 (0.0–13.4)	11.7 (0.0–23.8)
Un/underinsured flood	2.4 (0.0–3.9)	6.2 (2.9–8.8)	6.6 (3.4–10.8)	8.2 (3.5–9.6)	11.5 (4.3–20.1)	2.4 (0.0–3.9)	1.3 (0.0–2.0)	2.6 (0.0–4.1)
<i>Institutional stress</i>								
Total public burden	2.7 (0.0–1.7)	7.1 (3.3–11.0)	7.8 (4.0–13.9)	9.6 (4.1–12.3)	14.9 (5.1–29.7)	3.1 (0.0–2.7)	5.1 (0.0–2.5)	1.6 (0.0–0.5)
FHCF shortfall	0.3 (0.0–0.0)	1.0 (0.4–1.6)	1.1 (0.6–2.1)	1.5 (0.6–2.0)	2.5 (0.8–5.1)	0.4 (0.0–0.0)	0.7 (0.0–0.0)	0.2 (0.0–0.0)
FIGA residual	1.3 (0.0–1.0)	3.4 (1.6–5.2)	3.8 (1.9–6.6)	4.7 (2.0–6.0)	7.3 (2.5–14.3)	1.1 (0.0–0.7)	2.0 (0.0–1.0)	0.8 (0.0–0.3)
Citizens deficit	0.7 (0.0–0.7)	1.8 (0.9–2.8)	2.0 (1.0–3.4)	2.4 (1.0–3.0)	3.5 (1.3–6.9)	1.3 (0.0–2.1)	1.2 (0.0–1.6)	0.5 (0.0–0.2)
NFIP Treasury borrowing	0.3 (0.0–0.0)	0.8 (0.4–1.4)	0.9 (0.5–1.7)	1.0 (0.4–1.4)	1.7 (0.6–3.4)	0.3 (0.0–0.0)	1.2 (0.0–0.0)	0.2 (0.0–0.0)

Table S5: Probabilistic exceedance of systemic insurance stress thresholds across climate and policy scenarios. Annual exceedance probabilities (percent) of systemic stress thresholds for private insurers, public and quasi-public institutions, and aggregate fiscal impact, estimated from 10000 simulated tropical cyclone seasons. Results are shown for present-day conditions, mid-century (2050) and end-of-century (2100) climate scenarios under SSP2-4.5 and SSP5-8.5, as well as illustrative market and policy interventions evaluated under present-day climate forcing. Values denote mean probabilities, with uncertainty ranges (10th–90th percentile) in parentheses.

Metric (%)	Baseline	2050 SSP2-4.5	2050 SSP5-8.5	2100 SSP2-4.5	2100 SSP5-8.5	Market Exit	Insurance Penetration	Building Codes
Defaults > 10	11.4 (10.9–11.8)	17.7 (12.6–20.6)	18.8 (13.1–22.2)	20.2 (13.5–21.3)	22.7 (14.6–27.3)	10.3 (9.9–10.7)	9.7 (9.3–10.0)	9.2 (8.8–9.6)
Single Deficit > \$1B	7.2 (6.9–7.5)	11.5 (7.9–14.2)	12.2 (8.6–15.9)	13.5 (8.8–15.1)	16.6 (9.9–22.8)	6.5 (6.2–6.8)	8.2 (7.9–8.6)	5.6 (5.3–5.9)
FHCF > 100% Cap	0.8 (0.7–0.9)	0.9 (0.7–1.1)	1.0 (0.7–1.2)	1.0 (0.7–1.1)	1.2 (0.8–1.6)	0.7 (0.6–0.8)	1.2 (1.0–1.3)	0.5 (0.4–0.6)
FIGA > 100% Capacity	13.6 (13.2–14.1)	22.1 (15.1–27.5)	23.3 (16.6–30.9)	26.0 (17.0–29.4)	32.3 (19.0–45.3)	12.8 (12.3–13.2)	13.4 (13.0–13.9)	11.5 (11.1–11.9)
Citizens > 100% Capacity	9.5 (9.2–9.9)	15.1 (10.4–18.8)	16.1 (11.2–20.8)	17.3 (11.5–19.4)	21.0 (12.6–29.5)	13.0 (12.6–13.4)	11.8 (11.3–12.2)	7.9 (7.6–8.3)
NFIP > 200% Annual Premium	5.0 (4.8–5.3)	5.9 (4.4–6.9)	6.1 (4.6–7.5)	6.6 (4.7–7.2)	7.7 (5.0–10.0)	5.0 (4.8–5.3)	9.3 (8.9–9.7)	4.0 (3.7–4.2)
Public Burden > 1% FL GDP	3.7 (3.5–3.9)	4.3 (3.2–5.1)	4.5 (3.4–5.5)	4.9 (3.4–5.3)	5.6 (3.7–7.3)	4.3 (4.0–4.5)	5.6 (5.3–5.9)	2.4 (2.2–2.6)
Public Burden > 10% FL GDP	0.1 (0.1–0.2)	0.2 (0.1–0.2)	0.2 (0.1–0.2)	0.2 (0.1–0.2)	0.2 (0.1–0.3)	0.2 (0.1–0.3)	0.7 (0.6–0.8)	0.0 (0.0–0.1)

Table S6: Sensitivity of model outputs to the insured wind loss fraction. Mean values (in \$B; insurer defaults reported as counts) for each output metric across five fixed values of the insured wind fraction f . The table also reports the relative change compared to the reference case ($f = 0.4$, the mean of the baseline Beta(4, 6) prior) and the approximate log–log elasticity ϵ evaluated at $f = 0.4$. Metrics with $\epsilon \approx 0$ are invariant to the insured fraction by construction; $\epsilon = 1$ indicates proportional scaling; and $\epsilon > 1$ indicates amplification through the insurance system.

Metric	Mean value (\$B)					Change vs. $f=0.4$				ϵ
	$f=0.1$	$f=0.2$	$f=0.3$	$f=0.4$	$f=0.5$	$\Delta_{0.1}$	$\Delta_{0.2}$	$\Delta_{0.3}$	$\Delta_{0.5}$	
<i>Loss decomposition</i>										
Wind insured — private	1.36	2.72	4.08	5.44	6.80	-75%	-50%	-25%	+25%	+1.00
Wind insured — Citizens	0.27	0.53	0.80	1.07	1.34	-75%	-50%	-25%	+25%	+1.00
Wind un/underinsured	10.26	9.12	7.98	6.84	5.70	+50%	+33%	+17%	-17%	-0.66
<i>Institutional stress</i>										
FHCF shortfall	0.02	0.10	0.22	0.36	0.50	-95%	-74%	-39%	+39%	+1.60
FIGA residual deficit	0.15	0.46	0.84	1.27	1.72	-88%	-64%	-34%	+36%	+1.40
Citizens residual deficit	0.12	0.29	0.49	0.71	0.94	-84%	-60%	-31%	+32%	+1.28
<i>Capital / defaults</i>										
Insurer defaults (count)	0.8186	1.4122	1.8586	2.1992	2.4831	-63%	-36%	-15%	+13%	+0.57
Largest entity deficit	0.05	0.13	0.22	0.32	0.43	-84%	-59%	-31%	+32%	+1.25

Table S7: Relative contributions of hazard variability and parameter uncertainty to model output variance. Values of η^2 from a one-way ANOVA applied to a nested Monte Carlo design (300 seasons \times 50 independent parameter draws per season), measuring the fraction of total variance attributable to between-season hazard differences versus within-season parameter uncertainty. $\eta^2 \geq 0.95$ for all non-flood metrics indicates that hazard realization dominates; the lower values for flood-linked metrics reflect the wind/water share Beta prior, which controls how much total damage is routed to NFIP versus private wind coverage.

Metric	η^2 (hazard)	$1 - \eta^2$ (parameters)
<i>Loss decomposition</i>		
Private insurer wind losses	0.976	0.024
Citizens wind losses	0.964	0.036
NFIP flood (insured)	0.772	0.228
Un/underinsured wind	0.977	0.023
Un/underinsured flood	0.749	0.251
<i>Institutional stress</i>		
FHCF shortfall	0.944	0.056
FIGA residual deficit	0.965	0.035
Citizens residual deficit	0.954	0.046
NFIP Treasury borrowing	0.734	0.266
<i>Defaults</i>		
Insurer defaults (count)	0.990	0.010
Largest entity deficit	0.961	0.039

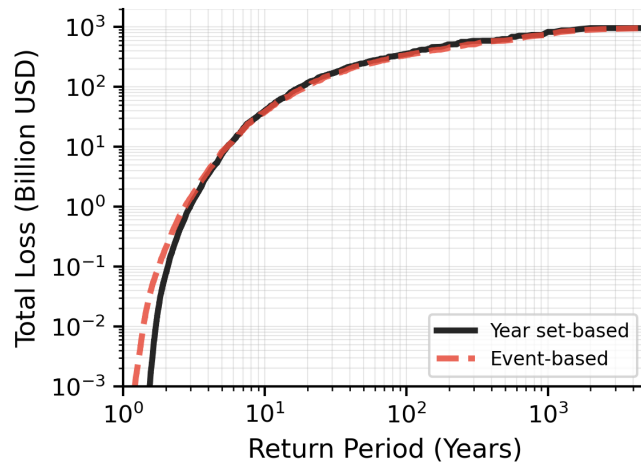


Fig. S1: Return period curves for total tropical cyclone losses in Florida. Event-based losses (red dashed line) and seasonal aggregate losses (solid black line) are shown. Event-based return periods are derived from the empirical exceedance distribution of single events in the historical tropical cyclone event set (8800 events covering 1980–2023; Section [Tropical cyclone track data](#)). Seasonal return periods are computed from the empirical exceedance distribution of aggregate losses across simulated 10000 tropical cyclone years (Section [Hazard and loss modeling](#)).

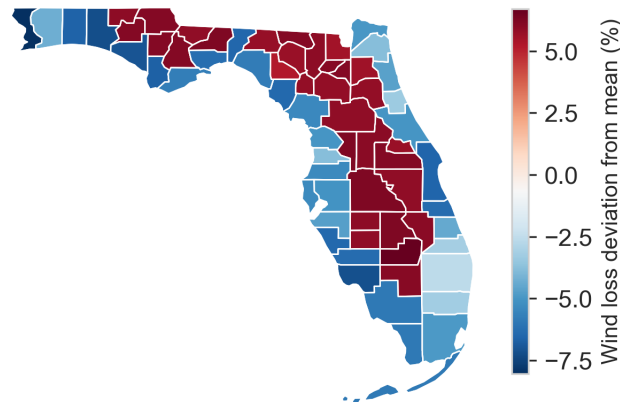


Fig. S2: County-level deviation in wind loss attribution across Florida. Percentage-point deviation of county-specific wind shares from the state-wide mean, derived from the upper 95th percentile of the compound hazard distribution in the synthetic tropical cyclone event set (cf. Methods Wind and flood loss estimation). Positive values indicate wind-dominated counties; negative values indicate relatively stronger flood contributions.